CUKUROVA UNIVERSITY
INSTITUTE OF NATURAL AND APPLIED SCIENCES

MSc THESIS

Husam Abdulkarem Abdulrazzaq AL-QADASI

CFD ANALYSIS of BIOMASS STEAM GASIFICATION in FLUIDIZED BED GASIFIER

DEPARTMENT OF MECHANICAL ENGINEERING

ADANA, 2019

ÇUKUROVA UNIVERSITY
INSTITUTE OF NATURAL AND APPLIED SCIENCES

CFD ANALYSIS of BIOMASS STEAM GASIFICATION in FLUIDIZED BED GASIFIER

Husam Abdulkarem Abdulrazzaq Al-Qadasi

MSc THESIS

DEPARTMENT OF MECHANICAL ENGINEERING

We certify that the thesis titled above was reviewed and approved for the award of degree of the Master of Science by the board of jury on 27/08/2019.

……..……..	……	……..……
Asst.Prof.Dr.Göktürk M.ÖZKAN	Prof. Dr. Hüseyin AKILLI	Assoc.Prof.Dr.Cihan YILDIRIM
SUPERVISOR	MEMBER	MEMBER

This MSc Thesis is written at the Department of Institute of Natural and Applied Sciences of Çukurova University.
Registration Number:

Prof.Dr. Mustafa GÖK
Director
Institute of Natural and Applied Sciences

This work was supported by Research Projects Center of Cukurova University
Project No: FYL-2018-11230

ABSTRACT

MSc THESIS

CFD ANALYSIS of BIOMASS STEAM GASIFICATION in FLUIDIZED BED GASIFIER

Husam Abdulkarem Abdulrazzaq AL-QADASI

CUKUROVA UNIVERSITY
INSTITUTE OF NATURAL AND APPLIED SCIENCES
DEPARTMENT OF MECHANICAL ENGINEERING

Supervisor : Asst. Prof. Dr. Gokturk Memduh Ozkan
Year: 2019, Pages: 56
Jury : Asst. Prof. Dr. Gokturk Memduh Ozkan
: Prof. Dr. Huseyin Akilli
: Assoc. Prof. Dr. Cihan Yildirim

In this study, a Multi-phase CFD model based on comprehensive pyrolysis chemical reaction model was developed to simulate the gasification process of biomass. Gasification temperature and steam to biomass ratio were the main parameters studied in this work. The present study filled the gap was left by the previous studies since it was able to analyze the effect of gasification temperature and steam to biomass ratio on the gasification products of almond shells. The effect of those parameters on produced gas composition, lower heating value of the produced gas, char yield, tar content, and tar components were studied. The obtained results of the base case agree to a good extent with the results of the experiment. Besides, the obtained results of the base case were compared with another CFD study to prove the accuracy of the present model.

Keywords: biomass, gasification, fluidized bed, syngas, CFD, SBR, char, LHV

ÖZ

YÜKSEK LİSANS TEZİ

AKIŞKAN YATAKLI GAZ DÖMÜŞTÜRÜCÜDE BUHARLI BİYOKÜTLE GAZLAŞTIRMA PROSESİNİN HAD ANALİZİ

Husam Abdulkarem Abdulrazzaq AL-QADASI

ÇUKUROVA ÜNİVERSİTESİ
FEN BİLİMLERİ ENSTİTÜSÜ
MAKİNE MÜHENDİSLİĞİ ANABİLİM DALI

Danışman: Dr. Öğr. Üyesi. Göktürk Memduh ÖZKAN
Yıl: 2019, Sayfa: 56
Jüri : Dr. Öğr. Üyesi. Göktürk Memduh ÖZKAN
: Prof. Dr. Hüseyin AKILLI
: Doç. Dr. Cihan YILDIRIM

Bu çalışmada, biyokütlenin gazlaştırma işlemini simüle etmek için kapsamlı piroliz kimyasal reaksiyon modeline dayanan Çok-Fazlı bir CFD modeli geliştirilmiştir. Gazlaştırma sıcaklığı ve buharın biyokütle oranı bu çalışmada çalışılan ana parametrelerdir. Bu çalışma boşluğu doldurdu deneysel çalışma tarafından bırakıldı, çünkü gazlaştırma sıcaklığı ve buharın biyokütle oranının gazlaştırma ürünleri üzerindeki etkisini analiz edebildi. Bu parametrelerin üretilen gaz bileşimi üzerindeki etkisi, üretilen gazın düşük ısıtma değeri, kömür verimi, katran içeriği ve katran bileşenleri incelenmiştir. Temel davadan elde edilen sonuçlar, deney sonuçlarına büyük ölçüde katılıyor. Ayrıca, temel durumdan elde edilen sonuçlar mevcut modelin doğruluğunu kanıtlamak için başka bir CFD çalışmasıyla karşılaştırılmıştır.

AnahtarKelimeler: biyokütle, gazlaştırma, akışkan yatak, syngas, CFD, SBR, LHV

EXTENDED SUMMARY

Recently, the planet faces a critical problem of global warming, which negatively and dangerously affects all organisms on earth. The use of fossil fuels is one of the main reasons for the exacerbation of this dangerous phenomenon, and therefore the need to use renewable and clean energy resources has emerged.

The use of renewable energy resources may solve many environmental and economic problems because these resources are available worldwide. Encouraging scientific research in these areas contributes to the protection of the climate of the earth.

Biomass energy is one of the most promising renewable energy sources in the world. The use of biomass energy can help to reduce environmental pollution by using unwanted residuals from industrial activities. The availability of biomass residuals in various countries has attracted the attention of many researchers around the world. The biomass gasification process is one of the most effective ways to utilize biomass energy.

The advantage of the gasification process is increasing the produced syngas through the reaction between the gasification agent and produced char. Gasification agent can be steam, oxygen or air. Some of the most important parameters in the gasification process are the gasification temperature and steam to biomass ratio (SBR).

A good estimation of optimum gasification temperature could help increase the efficiency of the gasification process by increasing produced syngas, hence the potential energy to be extracted from the biomass.

There are different types of gasifier reactor such as updraft gasifiers, downdraft gasifiers, circulating fluidized bed gasifiers, entrained flow gasifiers, and fluidized bed gasifiers. Fluidized bed gasifiers offer good mixing characters due to the movement of the bed material, thus the heat transfer rate increases.

In this study, the effect of gasification temperature on fluidized bed gasification process in terms of produced gas components, lower heating value of the produced gas, char yields, tar content, and tar components was studied using Computational Fluid Dynamics model. The effect of temperature on gasification was investigated at T = 950 K, 1043 K, and 1100 K.

The minimum fluidization velocity and the ratio of terminal velocity to minimum fluidization velocity were taken as U_{mf} = 0.075 m/s and U_{stean}/U_{mf} = 2.44, respectively.

In addition, the effect of steam to biomass ratio (SBR) on the previously mentioned parameters, which are produced gas components, lower heating value of the produced gas, char yields, tar content, and tar components, was also studied. The values of steam to biomass ratio was used in this study (SBR=0.8, SBR=1, and SBR=1.2).

The model was able to solve 36 equations simultaneously including continuity equations, momentum equations, energy equations and species equations for both solid and gas phase. In addition k-epsilon turbulence model and Eulerian-Eulerian, multi-phase model were adopted in this model.

The gasification modeling process was based on a comprehensive pyrolysis chemical reaction model ,which consist of two main stages. The first stage is the primary pyrolysis stage, which consist of sixteen chemical reactions. The second stage is the secondary pyrolysis stage or secondary tar cracking stage, which consist of ten chemical reactions. Crushed almond shells were used as a biomass feedstock, sand was used as bed material and steam was used as a gasification agent.

The results were validated with an experimental work of (Rapagna et al., 2000) and analyzed using a comparison of dry produced gas components, lower heating value of the produced gas, char yield and tar content between experimental work and the results obtained from numerical model, furthermore, the gained results were compared with the previous study done by (Eri et al., 2018).

The model was proved to obtain results which agree to a very good extent with the experimental work of (Rapagna et al., 2000), however, the obtained results were found to be more accurate than the model proposed by (Eri et al., 2018).

The effect of gasification temperature on the mole fraction of dry syngas, which is free of condensable gases and tar content. With the increase of the temperature above 1043 K, the rate of production of H_2 is higher than CO. For this reason, it is more practical to increase the gasification temperature when the aim is producing H_2. Besides, the gasification temperature has a negative effect on the mole fraction of both CO_2 and CH_4 in which their mole fractions are decreasing with increasing gasification temperature. In addition, the value of lower heating value (LHV), char yield, and tar content are decreasing with increasing gasification temperature.

It was found that as steam to biomass ratio (SBR) increases, both H_2 and CO mole fraction increase, which is agree with the results obtained by (Franco et al., 2003, Gungorl et al., 2011). On the other hand, as SBR ratio increases both CH_4 and CO_2 mole fraction decrease. LHV of the producer gas is reduced by increasing the SBR. In addition, with increasing SBR, char yeild increases and tar content decreases.

The effect of both gasification temperature and steam to biomass ratio (SBR) on the tar components was also studied. In this study C_2H_5OH, CH_3HCO, CH_3OH, CH_2O, $C_6H_6O_3$, and CH_3COCH_3 was considered as the tar component. The effect of secondary tar cracking reactions was obvious and noted.

In this study, the commercial CFD solver $ANSYS\ FLUENT$ 17 was used to develop a biomass gasification model based on a comprehensive model of pyrolysis. Results obtained from the numerical model were compared with the experimental results and some previous studies in terms of gas yield, lower heating value (LHV), char and tar yield.

The present study filled the gap was left by the previous studies since it was able to analyze the effect of gasification temperature and steam to biomass ratio on the gasification products of almond shells. Besides, the obtained results of the base case were compared with other computational fluid dynamics (CFD) study to prove the accuracy of the present model.

Studying the effect of equivalence ratio, the height of the bed, the material of the bed and geometry of the gasifier reactor is recommended of future studies. In addition, studying the hydrodynamic behavior of fluidized bed gasifier is recommended to improve and optimize the efficiency of the process.

ACKNOWLEDGMENTS

To my father Abdulkarem, how was the first supporter of mine and the one who believed on me when everyone did not. To my mother Najwa who was praying for me every time I talk to her. To my sisters Nashwa, Samah and Samara who made me feel that I am the best brother in the world, even if I am all away from them. To my brothers Nashwan, Wesam, and Mohammed, the men who took the responsibility of the family and were eager to keep me away from any disturbance during my study. To the best person in the world who endures my nervousness and who was beside me in the worst situations I had in my strangeness. To the best country to my heart, Yemen. This work is dedicated to all of you.

This work would not be done without the huge support of Asst. Prof. Dr. Gokturk M. OZKAN, the one who affect me in a very positive way. I was really lucky to work under his supervision. Also, I cannot forget Prof. Dr. Huseyin AKILLI, who was dealing with all his students as a father and the one who always comes to my mind whenever I face any problem. I will not forget anything of what he has done for me.

Finally, I would like to thank all my friends in Turkey from all over the world. I was very lucky to be a part of this international community. I have learned a thing from every one of you, so thank you for your contributions to my life.

CONTENTS **PAGE**

LIST OF TABLES **PAGE**

LIST OF FIGURES **PAGE**

LIST OF SYMBOLS AND ABBREVIATIONS

A : Pre-exponential factor

E : Activation energy

T : Temperature

g : Gas phase

s: Solid phase

α : Phase's volume fraction

ρ : Density

$\vec{u}$: Velocity vector

S : Interphase mass transfer terms

∇p : Pressure

K : Momentum exchange coefficient

$\vec{g}$: Acceleration

$\bar{\bar{\tau}}$: Second order stress tensor

H: Specific enthalpy

λ: Thermal conductivity

h_{gs} : Heat transfer coefficient

X : Mass fraction

R : Rate of formation

n : Species

C_D : Drag coefficient

d_s : Particle diameter

c_p : Specific heat

LHV : Lower heating value

SBR : Steam to biomass ratio

ABR : Air to biomass ratio

ER : Equivalence ratio

1. INTRODUCTION

Due to the low stocks of fossil fuels such as coal and oil, as well as the limited resources and environmental and climatic problems resulting from its use, which directly affect the lives of different organisms on the planet, the need to use renewable, unlimited and environmentally friendly sources of energy has emerged.

Biomass is one of the most promising renewable sources of energy used since ancient times as an energy source used in cooking, heating, and lighting. Among the many technologies to exploit biomass energy, gasification technology has emerged as one of the most effective and efficient techniques (Littlewood, 1977, Shadle et al., 2000, Phillips, 2006).

Gasification can be defined as a thermo-chemical process through which flammable gases such as H_2, CO, and CH_4 can be extracted from biomass in the presence of a gasification agent such as steam, air or oxygen. Gasification purposes are not limited only to syngas production which can be used as a source of energy, but it can also be used to produce many chemical feedstocks (Ku et al., 2015).

Interest in gasification began for the first time scientifically in 1659 by Thomas Shirley, who conducted the first investigation to produce the CH_4 using gasification technology (Sikarwar and Zhao, 2017). Attention to this technology continues to be developed to the present. Gasification products can replace conventional fuel sources since they can be used as fuel for heating, internal combustion engines or for generating electricity by gas turbines. Produced char can also be utilized as an alternative to coal. In addition, the produced gases can be used as raw materials for liquid fuels and some chemicals production (Kirkels and Verbong, 2011, Ferreira et al., 2009, Kırtay, 2011).

There are many types of gasification reactor such as upward draft, downward draft, cross draft, and fluidized bed gasifiers (Baruah and Baruah, 2014). Fluidized bed reactor is one of the most efficient types of gasification reactors, as it improves the rate of heat transfer and mass significantly, provides a better temperature control within the reactor and has good mixing characteristics (Kern et al., 2013, Li et al., 2004, Shen et al., 2008).

Bed material can be either inert such as sand or catalytic such as olivine (Rapagna et al., 2000). Bed material and its fluidized movement help increase the heat transfer rate to biomass and maintain a uniform temperature distribution inside the reactor. Many physical and chemical processes occur inside the gasification reactor such as drying, pyrolysis, combustion, gasification, tar cracking, as well as an infinite number of complex chemical reactions (Baruah and Baruah, 2014, Boroson et al., 1989).

During the drying stage, the moisture content of the biomass is eliminated. The higher the moisture content in the feedstock, the less efficient the process of gasification. This is due to the waste of part of the thermal energy in the evaporation process of moisture (Kaushal et al., 2011, Gungor, 2011).

The pyrolysis stage is one of the most important stages of the gasification process, during which long and complex hydrocarbon chains are cracked into smaller and less complex chains (Basu, 2010). Some researches have divided the process of pyrolysis into two stages(Blondeau and Jeanmart, 2012, Mellin et al., 2014). The first stage is the primary pyrolysis stage, during which char, syngas, and tar are produced. The second stage is secondary pyrolysis stage, during which the tar is cracked into non-condensable gases and char. In this study, a comprehensive two-stage pyrolysis chemical reaction model has been used to develop the numerical model. However, the chemical reactions of pyrolysis are still complex and not fully understood (Calonaci et al., 2010).

During the gasification stage, the char reacts with the gasification agent and gases produced at the pyrolysis stage to increase the production syngas which is a combination

of H_2, CO and CH_4. There are two types of chemical reaction in the gasification stage, which are homogenous and heterogonous reactions.

Recently, computational fluid dynamic models have become widely popular and used to model complex systems with a capability to obtain more accurate results, as they are constantly under development and improvement (Papadikis et al., 2010, Ku et al., 2013). What helps to make it more practical is the rapid development of computer capabilities which in turn contributes to reducing the computational costs.

Computational fluid dynamic models have demonstrated their ability to save effort and money in comparison to laboratory experiments. In numerical models, an infinite number of modifications can be made to the various parameters of the system and their impact can be studied on the obtained results using only a computing machine. Unlike laboratory experiments that require a lot of equipment, devices, and materials that may be unavailable or difficult to obtain.

In general, the approaches used for modeling fluidized bed gasification systems can be classified into Eulerian-Eulerian approach and Eulerian-Lagrangian approach. For the Eulerian-Lagrangian approach, the characteristics of the gas phase are studied through a control volume, while the solid phase characteristics are studied by tracking each particle individually as it moves through space and time (Snider et al., 2011, Xie et al., 2012, Ku et al., 2015). On the other hand, the Eulerian-Eulerian approach deals with both gas phase and solid phase as interpenetrating continuum (Gerber et al., 2010, Wang et al., 2009, Xie et al., 2014).

Using Eulerian-Lagrangian approach, the results obtained could be more accurate, but due to limited computing capabilities available, it is difficult to adopt the Lagrangian approach. This is because the tracking process of each particle individually requires very high specifications for the computing machine. For example, in a study conducted by (Zhou et al., 2005), which investigates the coal combustion, they were able to make a

simulation of only two seconds using 20 particles of coal and 2,000 particles of sand by adopting the Lagrangian approach.

In this study, the commercial CFD solver $ANSYS\ FLUENT$ 17 was used to develop a biomass gasification model based on a comprehensive model of pyrolysis. Results obtained from the numerical model were compared with the experimental results available within the literature (Rapagna et al., 2000) and some previous studies in terms of gas yield, lower heating value (LHV), char and tar yield. The effects of some parameters on the results of the numerical model were also studied and analyzed.

2. LITERATURE REVIEW

Thermodynamic equilibrium model has been developed by (Schuster et al., 2001) to simulate a heat and power plant based on a fluidized bed gasifier. The effect of many parameters on the products of the gasification process and the lower heating value of the produced gas was studied. The results of the model show that with high temperature the concentration of both H_2 and CO increases while the concentration of both CO_2 and CH_4 decreases. The study did not show a clear effect of temperature on LHV.

Using ASPEN PLUS simulator, a comprehensive process model was developed by (Nikoo and Mahinpey, 2008) for gasification biomass. Through the model, the effect of both temperature and SBR on the components of the producer gas and carbon conversion efficiency was studied. As the temperature increases, H_2 production increases and carbon conversion becomes more efficient. However, CO production decreases. Also with the increasing SBR, the production of both H_2 and CO_2 is increasing while both CO_2 concentration and carbon conversion efficiency is decreasing. In general, the results obtained from the model lack accuracy as they failed to predict some trends.

(Kumar et al., 2009) study focused on the effect of both temperature and SBR on the concentration of H_2, CH_4 and char experimentally. This study showed that with an increase in temperature, the concentration of H_2 increases significantly, while there is no effect of SBR on H_2 concentration. On the other hand, the increase in temperature reduces the concentration of CH_4 and carbon conversion efficiency, while the concentration of CH_4 increased with increasing SBR. The study failed to determine any behavior of CO concentration under both parameters. In addition, the study showed that as SBR increases, the amount of char increases, but it wasn't able to determine any pattern of the effect of temperature on the amount of char.

To predict the products of the gasification process a thermodynamic equilibrium model has been developed by (Karmakar and Datta, 2011). The results of the model were compared with the results of the laboratory experiments. Laboratory results and model results showed that as the temperature increases, the concentration of both H_2 and CO increases, while CH_4 and CO_2 concentrations appeared in the opposite direction. The effect of SBR on the resulting gas components was also studied. The result of H_2 concentration was well consistent with the laboratory results but the accuracy of the results of both CO and CO_2 concentrations were poor. In addition, the model failed to determine the true trend of CH_4 concentration. The results of the model show that as the SBR increases, CH_4 concentration increases and this is contrary to the laboratory results.

An experimental study conducted by (Chang et al., 2011) to investigate the gasification of the biomass to produce the syngas. The experiment results showed that as the temperature increases the concentration of the syngas and its LHV are increasing. However, this study failed to determine the obvious effect of SBR on both the concentration of the syngas and its LHV.

(Xue and Fox, 2014) study demonstrates the CFD model of gasification using fluidized bed gasifier. The kinetic theory of granular flow was used for modeling the physical and chemical processes of the solid phase and its interaction with the gas phase. The gasification agent was the air instead of steam in this study. The results of the simulation showed that with higher temperatures, the production of both CO and CO_2 increases whereas the production of H_2, CH_4 tar, and char decreases. The effect of the air to biomass ratio on H_2 production was positive. In contrast, the CO, CO_2, CH_4 and tar decreased with increasing ABR.

Lagrangian-Eulerian method has been used by (Ku et al., 2015), to model the solid-gas phases. The gasification agent was steam and several parameters have been studied such as reactor temperature, steam to biomass ratio and biomass injection position. The

results showed that a higher temperature is preferable to produce H_2 and CO. Increasing of steam to biomass ratio increases both of H_2 and CO_2 concentration while decreases CO concentration.

Two diminsional, CFD model has been developed by (Ismail et al., 2016) using Eulerian-Eulerian method to model gas-solid phases. The model can predict the effect of equivalence ratio in the gasification temperature and provide sensitive analysis of the model of produced syngas composition in addition to higher heating value and cold gas efficiency. The high moisture content of the feedstock has a bad effect on cold gas efficiency and HHV. The effect can be decreased by increasing the equivalence ratio. Higher ER increases CO_2 and NO_2 concentration and decreases H_2, CO, and CH_4. Increasing moisture content increases the H_2 due to the water-gas shift reaction.

A comprehensive model was developed by (Liu et al., 2016) using the multi-phase approach to apply a parametric study to know the effect of some parameters on the producer gas components. The results of the study showed that as the temperature increases, the production of both H_2 and CO improves while the concentration of both CO_2 and CH_4 decreases. The results also showed that as SBR increases both H_2 and CH_4 concentrations increase. However, the study could not clearly determine the effect of SBR on both CO and CO_2. The study showed that the effect of SBR on the producer gas components is much lower compared to the effect of temperature.

The effect of both temperature and steam biomass ratio have been studied by (Eri et al., 2018). The simulation proceeds with a temperature of (950 K, 1000 K, 1045 K, and 1100 K) and steam to biomass ratio of (.8, .9, 1, 1.1 and 1.2). As the temperature increases the mole friction of H_2 increase, while CH_4 and CO_2 decrease. The tar content decrease while the char yield increase with increasing the temperature. The effect of steam to biomass ratio was not obvious on syngas, tar content, char yield, and tar composition.

Gasification tests were performed in a pilot-scale fluidized bed gasifier by (Ismail et al., 2018), in order to and investigate the effect of gasification temperatures at 750 ºC, 800 ºC, and 850 ºC at a constant biomass flow rate of 45 kg/h. Both phases, solid and gaseous, were described using Eulerian-Eulerian approach. The produced results show the impact of the increased temperature in the lower heating value of the syngas. The tests carried out at 750 ºC shown an increase in CO_2 and N2 and a decrease of CO in the range of 5% compared to the tests carried out at 850 ºC. In addition, increased temperature favors a decrease in tar production in the thermal gasification process. Elevated temperatures tend to favor the thermal cracking reactions and increased CO concentration, which increase the calorific value of the synthesis gas.

A comprehensive CFD model was developed by (Qi et al., 2019) for the simulation of biomass gasification in a fluidized bed reactor. The results showed that as the temperature increases, the production of CO improves, while the concentration of CO_2 decreases. This is consistent with the laboratory results, but the model fails to predict the correct trend of H_2 concentrations. The laboratory and numerical results also showed no significant effect of temperature on the concentration of CH_4 On the other hand, both H_2 and CO_2 are increased with increased SBR, while the concentration of CO decreases.

3. MATERIAL and METHOD

3.1. Parameters and Material Characterization

The model developed in this study is based on the experimental work done by (Rapagna et al., 2000), which used steam as a gasifier agent. Table 3.1 summaries the main properties of bed material used.

Table 3.1. Main properties of bed material (Rapagna et al., 2000)

Property	Bed material
Size distribution (mm)	
>0:780	0
0.780-0.655	0
0.655-0.550	5
0.550-0.463	20
0.463-0.390	29
0.390-0.328	24
0.328-0.275	14
0.275-0.231	7
0.231-0.165	1
Equivalent diameter (μm)	348
U_{mf} (m/s) (with steam at 820 C)	0.075
Particle density (kg/m^3)	2640

Table 3.2 summarizes the proximate analysis and ultimate analysis of almond shells in addition to lower heating value, density, and particle size. The biomass feed rate was fixed at 0.3 kg/h and the steam to biomass ratio SBR = 1. The experimental

test with sand as bed material was performed at temperature of 1043 K (Rapagna et al., 2000).

Table 3.2. Physical and chemical properties of biomass (Rapagna et al., 2000)

C (wt %)	46.65
H_2 (wt %)	5.55
O_2 (wt %)	38.74
N_2 (wt %)	9.06
Volatile matter (wt %)	72.45
Moisture (wt %)	7.90
Ash (wt %)	1.16
Fixed carbon (wt %)	18.49
LHV (kJ/kg)	18350
Density (kg/m^3)	1200
Particle size (μm)	1100

3.2. Mathematical and Numerical Modeling Approach

First, the pyrolysis and char gasification chemical reaction model will be discussed in details then the Eulerian-Eulerian multiple phase model will be discussed. All pyrolysis reactions are modeled with first-order Arrhenius kinetics depending on the pre-exponential factor (A), activation energy (E):

$$k = Ae^{-\frac{E}{RT}} \quad (1)$$

Where k is the reaction rate constant.

3.2.1. Pyrolysis Chemical Reactions Model

Pyrolysis is a thermo-chemical process in which the high complex hydrocarbon molecules of biomass are decomposed into smaller and more useful molecules in a form of gas, liquid, and char. The pyrolysis process usually occurs in the total absence of oxygen (Demirbas and Arin, 2002). Pyrolysis process of biomass is usually performed at relatively low temperature (237 K to 923 K) compared to gasification temperature (1073 K to 1273 K) (Basu, 2010).

3.2.2. Primary Pyrolysis Kinetic Scheme

The primary pyrolysis chemical reactions with the activation energies and reaction constants are shown in Table 3.3. (Ranzi et al., 2008, Calonaci et al., 2010). The reaction of moisture evaporation was taken from (Blondeau and Jeanmart, 2012). The corresponding reaction heat for pyrolysis reactions also summarized in the same table (Calonaci et al., 2010). In Table 3.3, cellulose and hemicellulose are indicated as $Cell$ and $HCell$ while the various types of lignin indicated as $LignC$ which is rich in carbon, $LignH$ which is rich in H_2 and $LignO$ which is rich in oxygen. Active Cellulose, which is obtained during the primary pyrolysis process as well as the rest of the components are considered as intermediate products. In the model, cellulose, hemicellulose, lignin, active cellulose, and char were modeled as solid species while the other components were modeled as a gaseous species. All of the produced gases from primary pyrolysis reactions are condensable gases, which form the tar except H_2, CO, CO_2, CH_4, C_2H_4, and H_2O, which are non-condensable gases (Susastriawan et al., 2017). In the thermogravimetric analysis, the initiation of pyrolysis occurs quickly for both hemicellulose (220 – 315 C) and cellulose (315 – 400 C). However, lignin needs a higher temperature to decompose (160 – 900 C) (Yang et al., 2007).

Table 3.3. Primary pyrolysis chemical reactions (Ranzi et al., 2008, Calonaci et al., 2010)

NO.	Reaction	$A\ (1/S)$	$E\ (kJ/mol)$
$R1$	$Cell \rightarrow 5H_2O + 6C$	8×10^7	125.5
$R2$	$Cell \rightarrow CellA$	8×10^{13}	192.5
$R3$	$CellA \rightarrow LVG$	$4T$	41.8
$R4$	$CellA \rightarrow 0.16\,CO_2 + 0.23\,CO + 0.9H2O + 0.1\,CH_4 + 0.61C + 0.25C_6H_6O_3 + 0.2CH_3COCH_3 + 0.2CH_3HCO + 0.25C_2H_2O_2 + 0.95HAA$	1×10^9	133.9
$R5$	$HCell \rightarrow 0.4HCell1 + 0.6HCell2$	1×10^{10}	129.7
$R6$	$HCell1 \rightarrow 0.75H_2 + 0.8\,CO_2 + 1.4CO + 0.5CH_2O$	3×10^9	113
$R7$	$HCell1 \rightarrow Xylan$	$3T$	46
$R8$	$HCell2 \rightarrow CO_2 + 0.5\,CH_4 + 0.25C_2H_4 + 0.8CO + 0.8H_2 + 0.7CH_2O + 0.25CH_3OH + 0.125C_2H_5OH + 0.125H_2O + C$	1×10^{10}	138.1
$R9$	$LignC \rightarrow 0.35LignCC + 0.1pCoumaryl + 0.08C_6H_5OH + 0.41C_2H_4 + H_2O + 0.495\,CH_4 + 0.32CO + CO + H_2 + 5.735C$	4×10^{15}	202.9
$R10$	$LignH \rightarrow LignOH + CH_3COCH_3$	2×10^{13}	156.9
$R11$	$LignO \rightarrow LignOH + CO_2$	1×10^9	106.7
$R12$	$LignCC \rightarrow 0.3pCoumaryl + 0.2C_6H_5OH + 0.35Acrylic - acid + 0.7H_2O + 0.65\,CH_4 + 0.6C_2H_4 + 1.8CO + H_2 + 6.4C$	5×10^6	131.8

$R13$	$LignOH \rightarrow$ Lign+H2O + CH_3OH +0.45 CH_4 + 0.2C_2H_4 + 2CO + 0.7H_2 + 4.15C	3×10^3	125.5
$R14$	$Lign \rightarrow Lumped - phenol$	$8T$	50.2
$R15$	$Lign \rightarrow H_2O$+2CO + 0.2CH_2O + 0.4 CH_3OH + 0.2 CH_3HCO + 0.2 CH_3COCH_3 + 0.6 CH_4 + 0.65C_2H_4 + 0.5H_2 + 5.5C	1.2×10^9	125.5
$R16$	$H_2O(l) \rightarrow H_2O(g)$	$5.3x10^{10}$	88

3.2.3. Secondary Pyrolysis Reactions Scheme

Primary pyrolysis process produces complex, heavy molecular gaseous species which can be condensed. During the residence of this species inside the gasifier and its flow through the bed material, tar undergoes a cracking process in which the heavy, condensable gaseous could be degraded to lighter and non-condensable gases (Xue and Fox, 2014).

According to (Fagbemi et al., 2001), the tar cracking process proceeds at a temperature higher than 500 C. The long residence time of chat inside the gasifier and its contact with char are important parameters that affect the tar cracking process (Fagbemi et al., 2001). Also, the gasification temperature plays an important role in tar decomposition as the decomposition increases as temperature increases. The mechanism of secondary pyrolysis is not understood yet because of the complexity of its reactions (Gómez-Barea and Leckner, 2010). In this study, the secondary pyrolysis reaction scheme has been taken from (Blondeau and Jeanmart, 2012) with hypothetical values for activation energy and pre-exponential factor from (Park et al., 2010) and summarized in Table 3.4. From the reactions listed in Table 3.4, we

can see that some reactions are contributing to char yield as the tar cracking reactions proceed.

Table 3.4. Secondary pyrolysis chemical reactions (Blondeau and Jeanmart, 2012, Park et al., 2010)

NO.	Reaction	A	$E\ (kJ/mol)$
$R17$	$C_6H_6O_3 \rightarrow 3\,CO + 1.5C_2H_4$	4.28×10^6	108
$R18$	$CH_3COCH_3 \rightarrow 0.5\,CO_2 + 0.5H_2 + 1.25C_2H_4$	4.28×10^6	108
$R19$	$pCoumaryl \rightarrow CO_2 + 2.5C_2H_4 + 3C$	4.28×10^6	108
$R20$	$C_6H_5OH \rightarrow 0.5\,CO_2 + 1.5C_2H_4 + 2.5C$	4.28×10^6	108
$R21$	$Xylan \rightarrow 2\,CO_2 + H_2 + 1.5C_2H_4$	4.28×10^6	108
$R22$	$LVG \rightarrow 2.5\,CO_2 + 1.5H_2 + 1.75C_2H_4$	4.28×10^6	108
$R23$	$HAA \rightarrow 2\,CO + 2H_2$	4.28×10^6	108
$R24$	$C_2H_2O_2 \rightarrow 2CO + H_2$	4.28×10^6	108
$R25$	$Lumped - phenol \rightarrow 2\,CO_2 + 3C_2H_4 + 3C$	4.28×10^6	108
$R26$	$Acrylic - acid \rightarrow CO_2 + C_2H_4$	4.28×10^6	108

3.2.4. Heterogeneous Chemical Reaction Model

Devolatization of biomass, which occurs during the pyrolysis process, converts the biomass particles to a mixture of gases and light char. Produced char consists primly of carbon and ash. The oxygen supply to the gasifier should be limited in order to prevent combustion. Many studies conclude that the heterogenous reactions between non-condensable gases inside the gasifier and char are very complex and not fully understood yet (Di Blasi, 2009, Ismail et al., 2016). In addition, heterogonous reactions are slower than homogenous ones (Xue and Fox, 2014, Gerber et al., 2010). Among the vast range of parameters, the particle's temperature and size, in addition to the gases' temperature

and components, appeared to be the most dominant parameters. Heterogeneous reactions and its kinetic parameters were taken from (Basu and Halder, 1989) and summarized in Table 3.5. The corresponding reaction rate conistant for heterogeneous reactions is

$$k = ATe^{-\frac{E}{RT}}$$

Table 3.5. Heterogeneous chemical reactions (Basu and Halder, 1989)

NO.	Reaction	A	$E(kJ/mol)$
$R27$	$C + CO_2 \rightarrow 2CO$ $+172.5\ kJ/mol$	3.42	130
$R28$	$C + H_2O \rightarrow CO + H_2$ $+131.3\ kJ/mol$	3.42	130
$R29$	$C + 2H_2 \rightarrow CH_4$ $-74.8\ kJ/mol$	3.42×10^{-3}	130

3.2.5. Homogeneous Chemical Reaction Model

The chemical reactions that describe the homogeneous gas-phase chemistry inside a gasifier reactor can be reached to hundreds of reactions (Gómez-Barea and Leckner, 2010, Fletcher et al., 2000), however, it is not possible to model all of those reactions due to the difficulty of calculating this huge number of coupled reactions. In order to simplify the homogeneous gas-phase reaction, four reactions were used to model the conversions in the gasifier reactor. Reactions $(R30)$ and $(R31)$ represent the steam reforming reactions while reactions $(R32)$ and $(R33)$ represent the forward and backward water-shift reactions. Both reactions and reaction rate expressions are summarized in Table 3.6. (Bustamante et al., 2004, Bustamante et al., 2005, Jones and Lindstedt, 1988)

Table 3.6. Homogeneous chemical reactions (Bustamante et al., 2004, Bustamante et al., 2005, Jones and Lindstedt, 1988)

NO.	Reaction	Reaction rate
$R30$	$CH_4 + H_2O \rightarrow CO + 3H_2 + 206\ kJ/mol$	$3 \times 10^8 . \exp(-\frac{15042}{T}) C_{CH4} C_{H2o}$
$R31$	$C_2H_4 + 2H_2O \rightarrow 2CO + 4H_2 + 212\ kJ/mol$	$3 \times 10^8 . \exp(-\frac{15042}{T}) C_{C2H4} C_{H2O}^2$
$R32$	$CO + H_2O \rightarrow CO_2 + H_2 - 41\ kJ/mol$	$7.68 \times 10^{12} . \exp(-\frac{36636}{T}) C_{CO}^{0.5} C_{H2o}$
$R33$	$CO_2 + H_2 \rightarrow CO + H_2O + 41\ kJ/mol$	$6.4 \times 10^{12} . \exp(-\frac{39259}{T}) C_{CO2} C_{H2}^{0.5}$

3.2.6. Multi-phase CFD Model

Both the gas phase and solid phase are represented as interpenetrating continuous phases using the Eulerian-Eulerian modeling approach (Anderson and Jackson, 1967, Drew, 1983, Ishii and Hibiki, 2010). The gas-phase which consists of all gaseous components is considered as primary phase, however, the solid phase which consists of cellulose, active cellulose, hemicellulose, lignin, and char is considered as a secondary phase. In addition, the bed material represented as an independent secondary solid phase. For each solid phase, all physical properties (particle diameter, density, etc.) and thermal properties (specific heat, thermal conductivity, etc.) are introduced. Tracking the volume fraction of the phases is the effective method for linking both primary and secondary phases. According to Equation 2, the summation of volume fractions of primary and secondary phases in the model must equal to unity:

$$\alpha_g + \sum_{m=1}^{M} \alpha_s = 1 \quad (2)$$

Where subscripts g and s refers to the gas and solid phase, respectively, M is the number of the phases, α_g is the gas phase's volume fraction and α_s is the solid phases' volume fractions. The kinetic theory of granular material is used to model the dynamic of solid transport, solid-solid, and solid-gas interactions inside the gasifier.

3.2.6.1. Gas-phase Governing Equations

A set of conservation equations for mass, momentum, and energy are used to model the gas phase (Xie et al., 2014, Couto et al., 2015, Chen et al., 2014). The continuity equation for the gas phase is

$$\frac{\partial(\alpha_g \rho_g)}{\partial t} + \nabla.(\alpha_g \rho_g \vec{u}_g) = S_{gs} \quad (3)$$

Where α, ρ, and $\vec{u}$ is the volume fraction, density and velocity vector respectively, S_{gs} are the interphase mass transfer terms from the solid phase due to reactions.

The momentum equation of the gas phase is

$$\frac{\partial(\alpha_g \rho_g \vec{u}_g)}{\partial t} + \nabla.(\alpha_g \rho_g \vec{u}_g \vec{u}_g) = -\alpha_g \nabla p + \alpha_g \rho_g \vec{g} - K(\vec{u}_g - \vec{u}_s) + S_{gs}\vec{u}_s + \nabla(\alpha_g \bar{\bar{\tau}}) \quad (4)$$

Where ∇p, K, $\vec{g}$, and $\bar{\bar{\tau}}$ is the pressure, momentum exchange coefficient, acceleration due to gravity and second order stress tensor respectively.

The energy equation of the gas phase is:

$$\frac{\partial}{\partial t}(\alpha_g \rho_g H_g) + \nabla(\alpha_g \rho_g \vec{u}_g H_g) = \nabla(\lambda_g \nabla T_g) + h_{gs}(T_g - T_s) + S_{gs}H_s \quad (5)$$

Where H, λ and T is specific enthalpy, thermal conductivity and temperature respectively, h_{gs} is the heat transfer coefficient between gas the phase and solid phase.

In this study, both the solid phase and the gas phase are consist of many species. For the gas phase, the species conservation is represented by Equation 6:

$$\frac{\partial}{\partial t}\left(\alpha_g\ \rho_g X_{gn}\right) + \nabla.\left(\alpha_g\ \rho_g \vec{u}_g X_{gn}\right) = R_{gn} \quad (6)$$

Where X_{gn} is the mass fraction and R_{gn} is the rate of formation of gas species n. For consistency, $\sum n = 1$

3.2.6.2. Solid-phase Governing Equations

Conservation equations for mass, momentum, and energy for solid-phase are similar to the equations used to model the gas phase (Xie et al., 2014, Couto et al., 2015, Chen et al., 2014). The continuity equation for solid-phase is

$$\frac{\partial(\alpha_s\rho_s)}{\partial t} + \nabla.(\alpha_s\rho_s\vec{u}_s) = -S_{gs} \quad (7)$$

The momentum equation of the solid phase is

$$\frac{\partial(\alpha_s\rho_s\vec{u}_s)}{\partial t} + \nabla.(\alpha_s\rho_s\vec{u}_s\vec{u}_s) = -\alpha_s\nabla p + \alpha_s\rho_s\vec{g} - K\left(\vec{u}_s - \vec{u}_g\right) - S_{gs}\vec{u}_s + \nabla(\alpha_s\bar{\bar{\tau}}_s) \quad (8)$$

Many studies (Loha et al., 2012, Sande and Ray, 2014) have concluded that the Gidaspow drag model is more convenient for dens bubbling fluidized bed, for this reason, the Gidaspow drag model (Gidaspow, 1994, Huilin et al., 2003) was used in this study. In addition, the solid-gas exchange coefficient, K_{sg}, is given by

When $\alpha_g > 0.8$

$$K_{sg} = \frac{3}{4} C_D \frac{\alpha_s\alpha_g\rho_g|\vec{u}_s-\vec{u}_g|}{d_s}\alpha_g^{-2.65} \quad (9)$$

When $\alpha_g \leq 0.8$

$$K_{sg} = 150\frac{\alpha_s(1-\alpha_g)\mu_g}{\alpha_g d_s^2} + 1.75\frac{\alpha_s\rho_g|\vec{u}_s-\vec{u}_g|}{d_s} \quad (10)$$

$$C_D = \frac{24}{\alpha_g Re_s}[1 + 0.15(\alpha_g Re_s)^{0.687}] \quad (11)$$

Where C_D, d_s, and Re_s is drag coefficient, particle diameter and Reynolds number respectively.

The energy equation of the solid-phase is

$$\frac{\partial}{\partial t}(\alpha_s\rho_s H_s) + \nabla(\alpha_s\rho_s\vec{u}_s H_s) = \nabla(\lambda_s\nabla T_s) + h_{sg}(T_s - T_g) - S_{gs}H_s \quad (12)$$

The heat transfer coefficient between the gas phase and solid phase depends on the Nusselt number, the volume fraction of both gas and solid phases, the thermal conductivity of the gas λ_g and the diameter of solid particles d_s. The expression of the heat transfer coefficient is given by

$$h_{gs} = h_{sg} = \frac{6\lambda_g\alpha_g\alpha_s Nu_s}{d_s^2} \quad (13)$$

The correlation of Nusselt number proposed by Gunn (Gunn, 1978) is used for solid-gas heat transfer coefficient.

$$Nu_s = \left(7 - 10\alpha_g + 5\alpha_g^2\right)\left(1 + 0.7Re_s^{0.2}Pr^{\frac{1}{3}}\right) + (1.33 - 2.4\alpha_g + 1.2\alpha_g^2)Re_s^{0.7}Pr^{\frac{1}{3}} \quad (14)$$

$$Re_s = \frac{\rho_g \phi |\vec{u}_s - \vec{u}_g| d_s}{\mu_g} \quad (15)$$

Where Pr is Prandtl number and ϕ is the void fraction in the bed.

For the solid-solid heat transfer coefficient, the proposed correlation of Nusselt number by Tomiyama is used (Tomiyama, 1998).

$$Nu_s = 2.0 + 0.15\, Re_s^{0.8}Pr^{\frac{1}{2}} \quad (16)$$

The species conservation equation for solid-phase has been driven in the same way of species conservation of gas phase. Rate of reaction and convection are considered in those equations.

$$\frac{\partial(\alpha_{s_m}\rho_{s_m}X_{s_m n})}{\partial t} + \nabla.\left(\alpha_{s_m}\rho_{s_m}X_{s_m n}\vec{u}_{s_m}\right) = R_{s_m n} \quad (17)$$

Where $X_{s_m n}$ is the solid mass fraction and $R_{s_m n}$ is the rate of formation of solid phase m, species n.

3.2.7. Computational Domain, Initial, and Boundary Conditions

In this study, two-dimensional geometry is used to represent the computational domain. As shown in Figure 3.1, the biomass is introduced to the gasifier through a side-inlet in the gasifier while the steam is introduced from the bottom of the gasifier. The flow domain consists of a rectangular reactor with a width of 60 mm and height of 600

mm where the biomass inlet is 20 mm, the steam inlet is 60 mm, and the gas outlet is 30 mm. Biomass particles and sand particles assumed to be spherical in the simulation.

Biomass particles' diameter is fixed to be 348 μm with a density of 1200 kg/m^3, while the sand particles' diameter is 1100 μm with a density of 2640 kg/m^3. The physical and chemical properties for both sand and biomass have been summarized previously in Table 3.1 and Table 3.2, respectively. In addition, the thermal properties of sand and biomass are summarized in Table 3.7. (Radmanesh et al., 2006, Ahuja et al., 1996), where c_p is the specific heat.

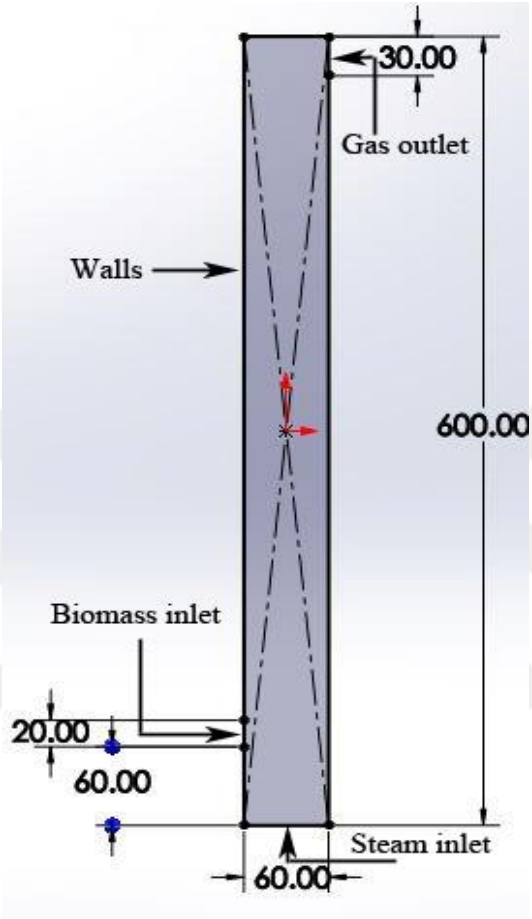

Figure 3.1. The geometry of Fluidized-bed gasifier

Table 3.7 Thermal properties of the solid phase (Radmanesh et al., 2006, Ahuja et al., 1996)

Property	Value
$c_{p,\text{shell}}$	2380 $J/(kg.K)$
λ_{shell}	0.158 $W/(m.K)$
λ_{sand}	0.2 $W/(m.K)$

$c_{p,\text{sand}}$	$860\ J/(kg.K)$

In the experimental setup, steam to biomass ratio (SBR) was 1 and the minimum fluidization velocity is U_{mf} = 0.075 m/s while ratio the of terminal velocity to minimum fluidization velocity is U_{stean}/U_{mf} = 2.44 which means that the inlet steam velocity is U_{stean} = 0.183 m/s (Rapagna et al., 2000). The boundary conditions of the base case are summarized in Table 3.8. In the simulation, the steam initially filled the gasifier and the no-slip wall boundary condition is applied to the walls.

Table 3.8. Boundary condition for the base case

Property	Value
U_{stean}	0.183 m/s
Steam to biomass ratio (SBR)	1
T_{wall}	1043 K
T_{stean}	1043 K
T_{shell}	600 K
T_{bed}	1043 K

In the base case, the initial temperature of the steam, which is the gasification agent, walls and sand was set to be 1043K. Meanwhile, the temperature of biomass was assumed to be preheated to 600 K. The atmosphere outlet boundary condition is adopted for the gas outlet, while the fluidized bed is initially packed at a solid fraction of 0.57 with a height of 125 mm.

3.2.8. Simulation Strategy

ANSYS FLUENT v17 was used to generate the model run the simulation. The time step size was set initially to 10^{-4} s, when the simulation became stable the time step size was changed to 10^{-3} s with a maximum 20 iterations per time step. The simulation was resolved for 10500 time-step to simulate the gasification for 10.5 seconds. Many studies have been conducted to study the mesh size effect on the accuracy of the obtained results. A coarse mesh, which has a big mesh size, can obtain an over-prediction of solid expansion height of the bed. On the other hand, the very fine mesh can increase the calculation cost and time with no further enhancement in the gained results (Chen et al., 2014). The mesh minimum orthogonal quality is 0.99994 , while the maximum skewness is 6.4×10^{-6}, furthermore, the maximum aspect ratio is 1.4. According to (Sande and Ray, 2014), the simulation results agree to a good extent with the experimental result when the grid size is 10 times bigger than the particle diameter. Therefore the total number of mesh was created to be 210000.

4. RESULTS and DISCUSSION

4.1. Time-Dependent Analysis

To prove the stability of the model, the produced gas compositions at the middle of the gasifier are monitored. Initially, the steam fills the gasifier reactor while other gas compositions do not exist, as seen in Figure 4.1, which represents the instantaneous mole fraction of steam as a unity while the other components are zero. As time goes on and the chemical reactions proceed, different products are produced and when those products reach the mid-line of the reactor, (at 1.5 seconds), the steam mole fraction starts to decline while the other components mole fractions start to increase. In addition, the mole fractions of both steam and CO are monitored at the gasifier outlet to recognize the point at which the model reaches a stable situation.

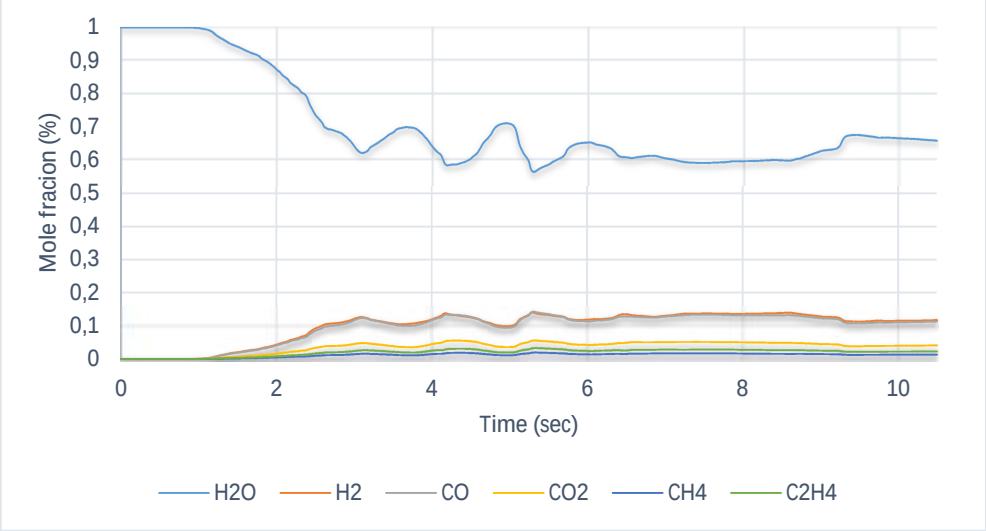

Figure 4.1. Instantaneous change of syngas mole fraction at the gasifier midline

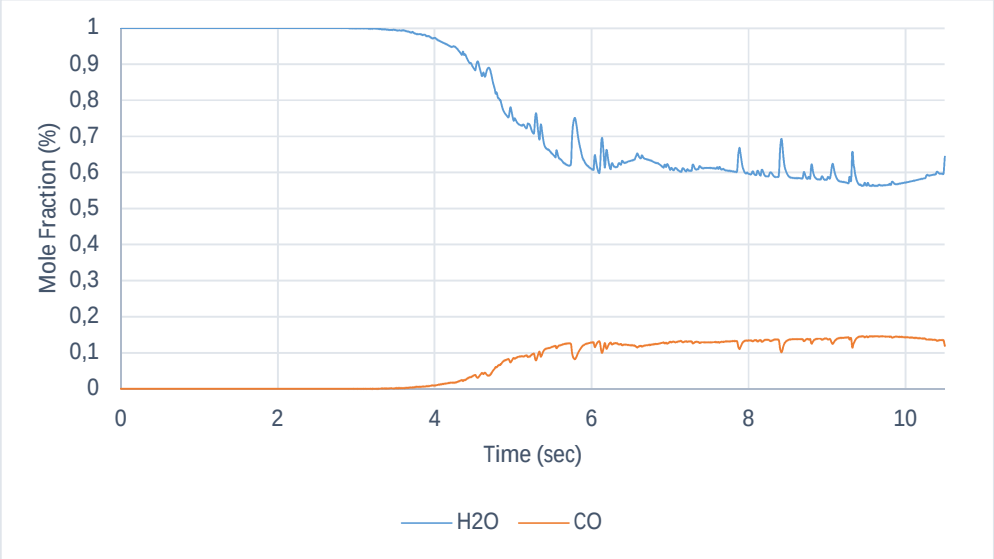

Figure 4.2. Instantaneous change of $\boldsymbol{H_2}$ and $\boldsymbol{CO}$ mole fractions at the gasifier outlet

From Figure 4.2., it is clearly evident that the model reaches a stable situation at 5.5 seconds, for this reason, the averaged values of all results are taking from 5.5 seconds to 10.5 seconds. The peaks appeared in Figure 4.2 is due to the reverse flow at the gasifier outlet. Figure 4.3. shows the fluidized bed movements involving the generation of bubbles. As represented in Figure 4.3, the bubbles at the bottom of the bed have small diameters and it became bigger as it go up.

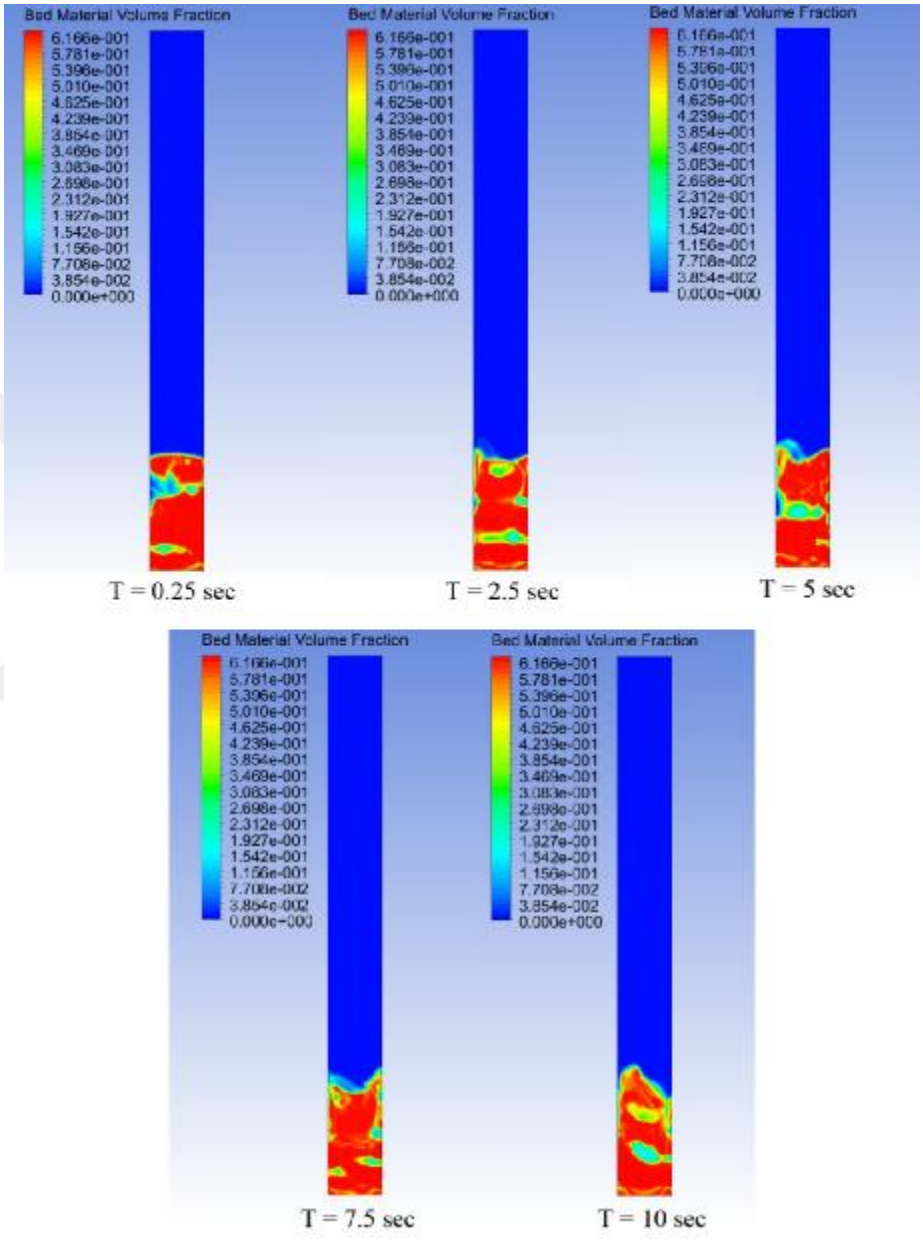

Figure 4.3. Bed material volume fraction at different time

Due to the secondary pyrolysis process, the complex and long-chained hydrocarbons from the primary are cracked to less complex products which form tar. In this study C_2H_5OH, CH_3HCO, CH_3OH, CH_2O, $C_6H_6O_3$, and CH_3COCH_3 was considered as the tar component. As $C_6H_6O_3$ and CH_3COCH_3 go up in the gasifier, they undergo a cracking reaction, for that reason the concentration of that two components decreases as they go up in the gasifier. Figure 4.4 illustrates the time-averaged mole fraction distribution of different tar components along the height of the gasifier.

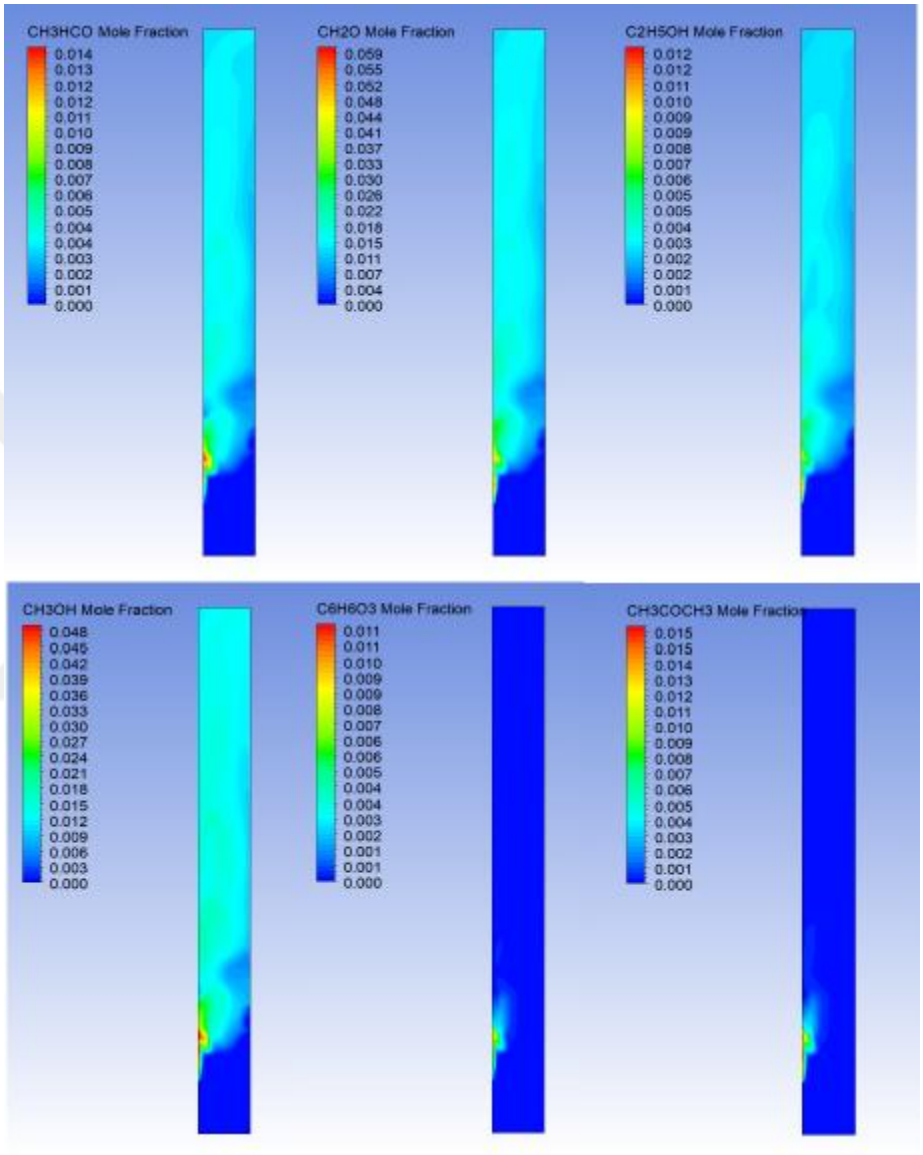

Figure 4.4. Time-averaged distributions of mole fraction of tar components

Due to the characteristics of the bubbles, segregation effects were shown in Figure 4.5. Represents the mole fraction of char. Char particles which have a lower density of the sand particle tend to float on the top of the bed inventory. It is observed that the char particles with low density are concentrated on the top of sand particles during the bubbling process.

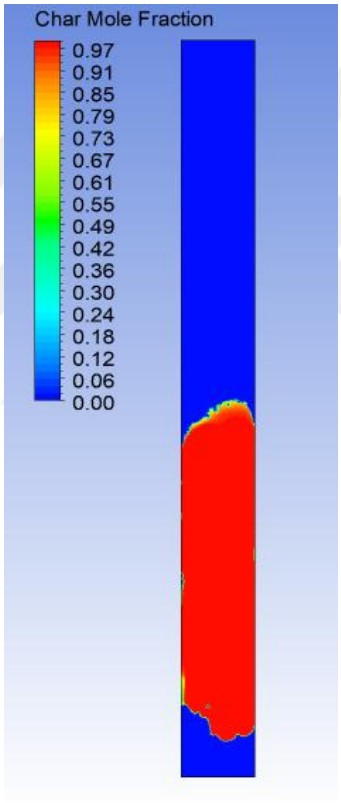

Figure 4.5. Time-averaged distribution of char mole fraction

4.2. Model Validation

Figure 4.6 represents the comparison between the experimental results (Rapagna et al., 2000), and numerical work of (Eri et al., 2018), with the obtained results from the base case, by means of the volume fraction of produced gas components at the gasifier outlet. The gas components considered here are the dry syngas components, which are not a part of tar components. Figure 4.6 shows that the simulation results are agreed to a good extent with the experimental results. Moreover, the obtained results are more accurate than the numerical results obtained by (Eri et al., 2018).

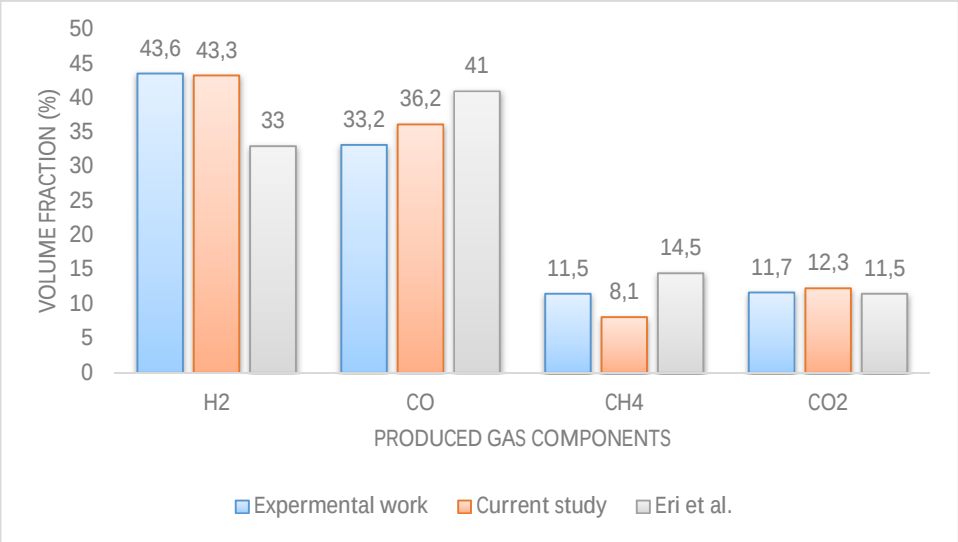

Figure 4.6. Comparison between the experimental results (Rapagna et al., 2000), obtained results and (Eri et al., 2018) results of produced gas components

To calculate the lower heating value of the syngas, only combustible components where considered which are H_2, CO, and CH_4 Equation 18 is used to calculate the lower heating value of the produced gas.

$$LHV = 12.64\varphi_{CO} + 10.8\varphi_{H_2} + 35.8\varphi_{CH_4} \quad (18)$$

Where φ is the mole fraction of the gas while the unit of LHV is MJ/Nm^3.

Figure 4.7 shows a comparison between the experimental work (Rapagna et al., 2000), current work and previous work done by (Eri et al., 2018) in terms of lower heating value, char yield and tar content. It is shown that the current work obtained more accurate results compared to the previous work for both char yield and tar content. The char yield was calculated by dividing char mass by the total mass of raw biomass entered the gasifier. The tar content was calculated by multiplying the concentration of all tar components by their molar weight then sum them together.

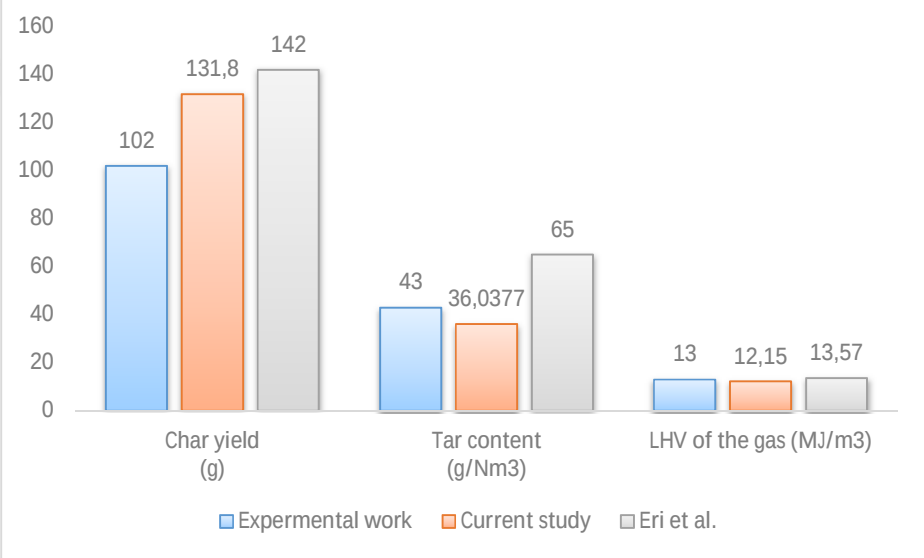

Figure 4.7. Comparison between the experimental results (Rapagna et al., 2000), obtained results and (Eri et al., 2018) results of values of tar content, char yield, and ***LHV***

According to the results presented and compared with previous experimental and numerical studies, the proposed steam gasification model is proved to be reasonable and accurate. The detailed results will be presented in the following sections to understand the effect of gasification temperature and SBR on the gasification process.

4.3. Effect of Temperature

During the study of the effect of gasification temperature, both sand temperature and wall temperature were set to be the same as the inlet steam temperature of all the cases. The temperature values studied in this work were taken as 950 K, 1043 K, and 1100 K.

Increasing gasification temperature helps to enforce the endothermic reactions. Therefore, the products of all homogenous and heterogeneous reactions (except of the forward water-shift reaction ($R32$) and methanation reaction ($R29$)) are increased with increasing the gasification temperature. Figure 4.8 represents the effect of gasification temperature on the mole fraction of dry syngas, which is free of condensable gases and tar content. With the increase of the temperature, the mole fraction of H_2 and CO increase, however, the rate of production of H_2 is higher than CO. For this reason, it is more practical to increase the gasification temperature when the aim is producing H_2. Besides, the gasification temperature has a negative effect on the mole fraction of both CO_2 and CH_4 in which their mole fractions are decreasing with increasing gasification temperature. The obtained results totally agree with many studies (Schuster et al., 2001, Karmakar and Datta, 2011, Liu et al., 2012, Wang et al., 2015).

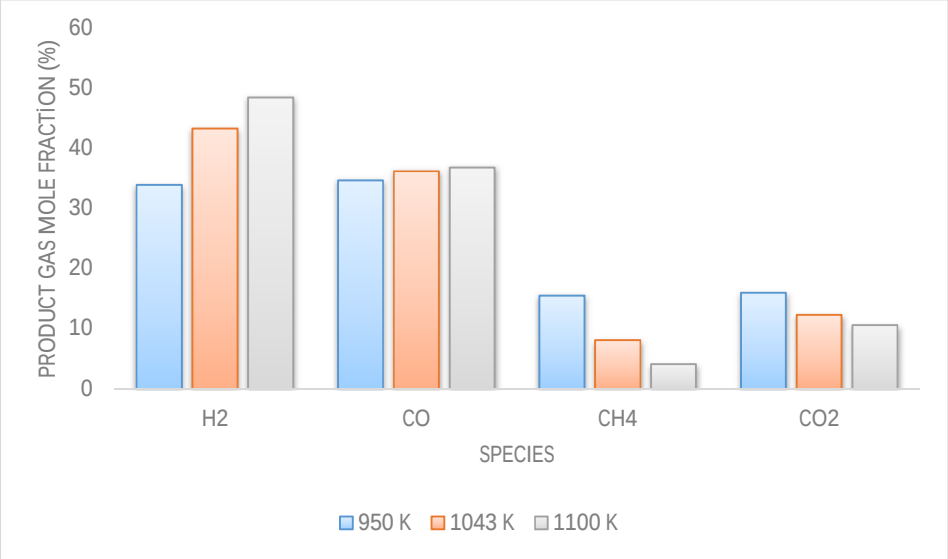

Figure 4.8. Effect of gasification temperature on produced gas components

The time-averaged distributions of H_2 and CO mole fraction along the gasifier reactor are shown in Figure 4.9 and Figure 4.10, respectively. It is obvious that with increasing the temperature, the rate of H_2 mole fraction production is higher than the the rate of CO mole fraction.

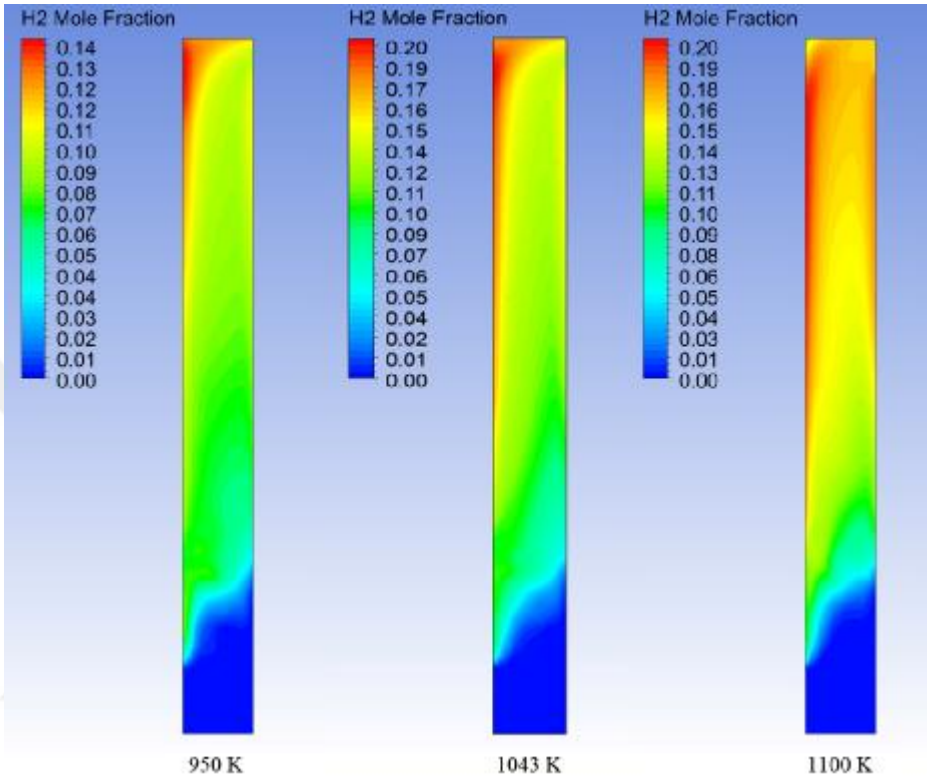

Figure 4.9. Time-averaged distribution of $\boldsymbol{H_2}$ mole fraction at 950 $\boldsymbol{K}$, 1043 $\boldsymbol{K}$ and 1100 $\boldsymbol{K}$

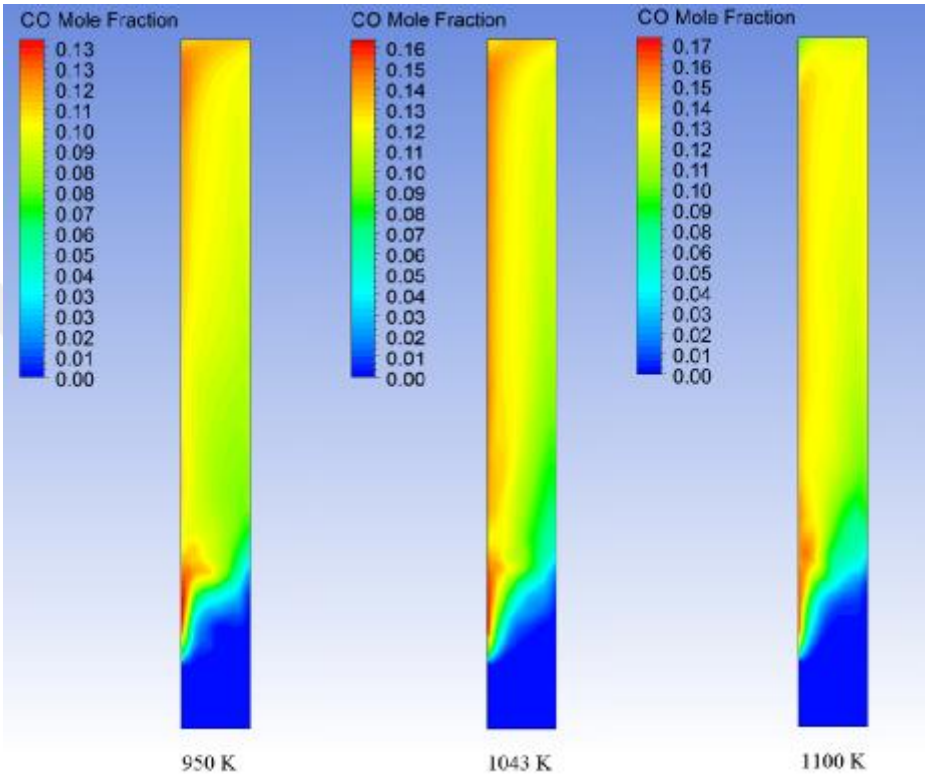

Figure 4.10. Time-averaged distribution of $\boldsymbol{CO}$ mole fraction at 950 $\boldsymbol{K}$, 1043 $\boldsymbol{K}$ and 1100 $\boldsymbol{K}$

In Equation 8, the coefficient corresponding to the CH_4 mole fraction is the highest and this means that the effect of mole fraction of CH_4 on the LHV in the most. As previously mentioned, the mole fraction of CH_4 shows a declined trend with increasing the temperature, therefore the value of LHV is decreasing with increasing gasification temperature. The effect of gasification temperature on the lower heating value of the syn-gas is shown in Figure 4.11. The obtained results show that as the gasification

temperature decreases below 1043 K, the effect on *LHV* is more obvious. On the contrary, as the gasification temperature increases above 1043 K, the effect on *LHV* is less.

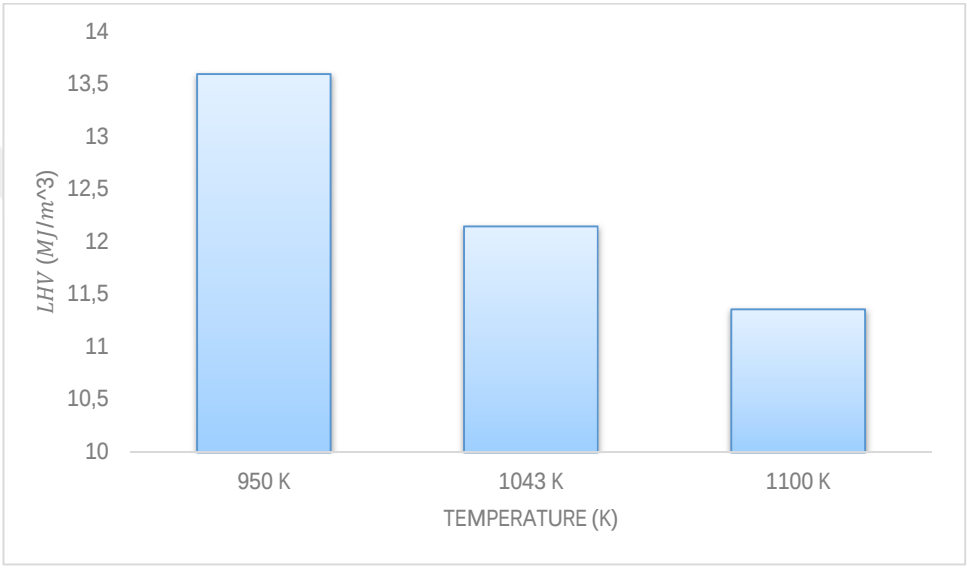

Figure 4.11. Effect of gasification temperature on ***LHV***

The gasification temperature effect on char yield and tar content is presented in Figure 4.12. The char yield reduces with increasing gasification temperature, this is due to the increase of reaction rates of heterogenous reactions. The obtained result agree with many literatures (Nikoo and Mahinpey, 2008, Karmakar and Datta, 2011, Kumar et al., 2009). In contrary, when the gasification temperature decreases the char yield increases due to the decreasing of chemical reaction rates char gasification.

As mentioned before, with increasing the gasification temperature the secondary pyrolysis reactions rate increases which means that the tar cracking process rate will increase. Therefore, the tar content shows a declined trend with increasing gasification

temperature. Figure 4.12 shows that at 950 K, the tar content has the highest value, while at 1100 K, the tar content has the lowest.

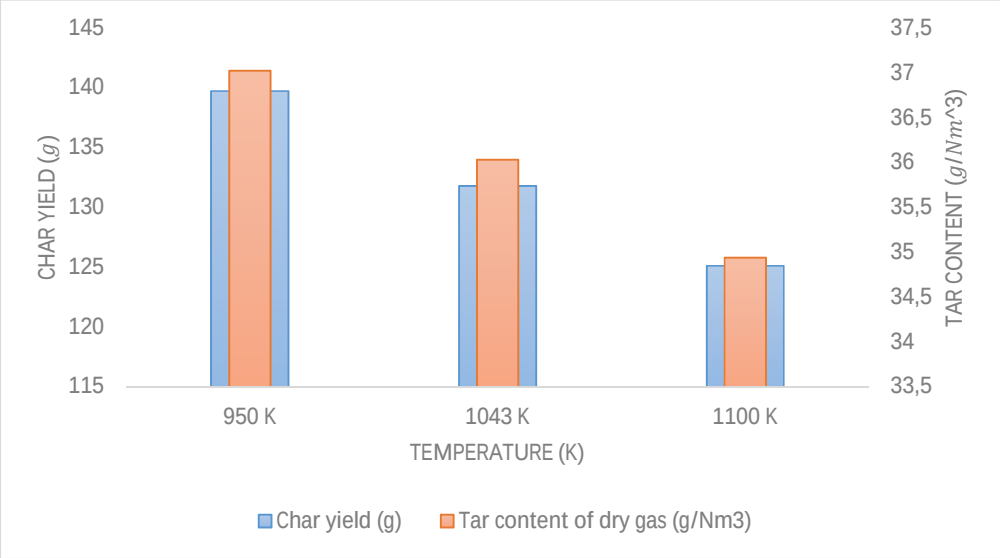

Figure 4.12 Effect of gasification temperature on char yield and tar content

In addition, to understand the effect of gasification temperature on the tar content, the effect on the mass fraction of the tar component was studied. Six tar components, which are condensable gases, were considered as the tar elements.

Four of the tar elements, which are CH_3HCO, CH_2O, C_2H_5OH, and CH_3OH are produced during the primary pyrolysis stage but it does not contribute in the secondary tar cracking stage, thus the mass fraction of those four elements increases as the gasification temperature increases. The reason for that is, as the temperature increases the reaction rates of primary pyrolysis reactions increase, so the rate of production of those elements increases. On the other hand, the remaining tar elements, which are $C_6H_6O_3$, and CH_3COCH_3, are exposed to the cracking process through secondary

pyrolysis reaction, which results in a decrease in their mass fraction with increasing the gasification temperature. CH_2O and CH_3OH form the highest percentage of tar mass fraction which contribute in 36.8% (at 950 K) to 38.1% (at 1100 K) and 39.4% (at 950 K) to 37.5% (at 1100 K) of tar mass fraction, respectively. Meanwhile, CH_3HCO forms 12.5% (at 950 K) to 13.4% (at 1100 K) of tar mass fraction. Furthermore, $C_6H_6O_3$ and CH_3COCH_3 are almost consumed in the tar cracking reactions when they reach the gasifier outlet. Figure 4.13 illustrate the temperature effects on the different tar components.

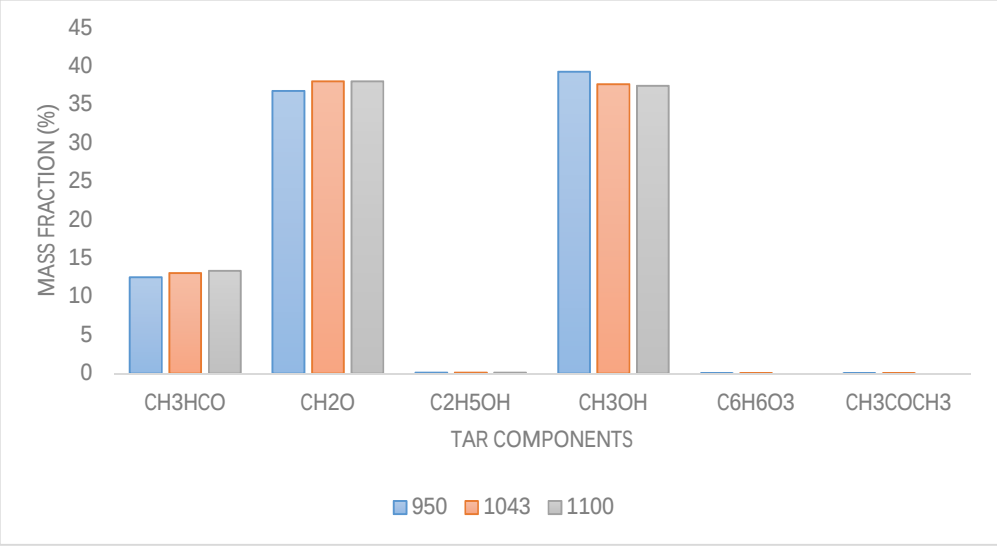

Figure 4.13. Effect of gasification temperature on tar components

4.4. Effect of SBR

In order to study the effect of steam to biomass ratio on the gasification process, different values of SBR were used, which are 0.8, 1, and 1.2, respectively. The gasification temperature was fixed to the base case temperature, which is 1043 K in the three cases. Unlike the method used in (Eri et al., 2018) to control the SBR, the biomass mass flow rate was fixed and the steam mass flow rate was modified. The method used in (Eri et al., 2018), which is modifying the biomass flow rate, would not provide accurate results due to the increase of biomass quantity which for sure will increase the char and produced gases in case of increase the SBR.

Nitrogen was used when SBR was set to 0.8 in order to make up the decrease the inlet steam velocity and keep the fluidization of the bed in a stable level. Nitrogen was selected because of its inert properties, which will not affect the chemical reactions.

Figure 4.14 demonstrates the effect of SBR on the producer gases at the outlet of the gasifier. It is clear that as SBR increases, both H_2 and CO mole fraction increase, which is agree with the results obtained by (Franco et al., 2003, Gungorl et al., 2011). This result is reasonable since the increase in SBR means increase to the quantity of steam inside the gasifier, and as a result the products of steam gasification reaction ($R28$), steam reforming reactions ($R30, R31$), and forward water shift reaction ($R32$) all increase consequently (Ku et al., 2015, Liu et al., 2016, Xie et al., 2012).

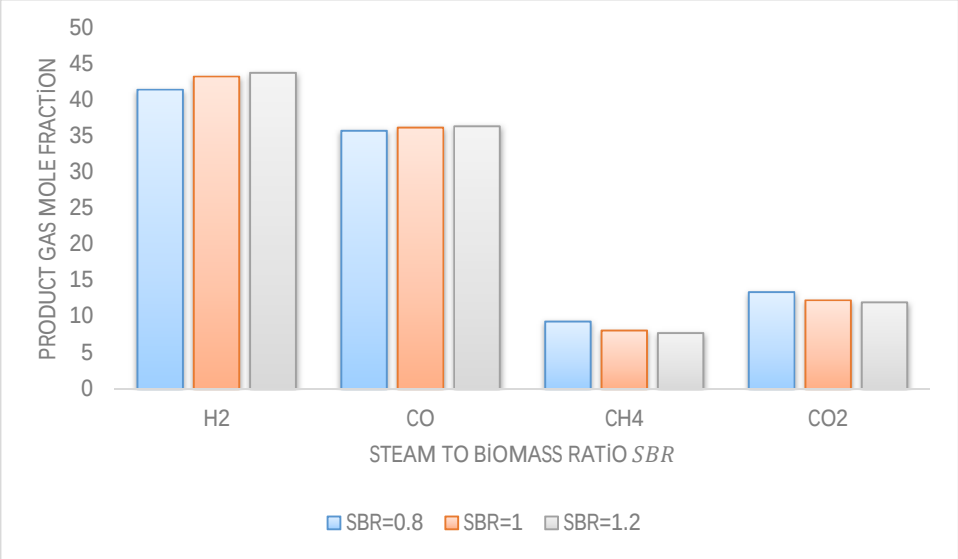

Figure 4.14. Effect of steam to biomass ratio on produced gas components

On the other hand, as SBR ratio increases both CH_4 and CO_2 mole fractions decrease because they are consumed at a higher rate in methane-steam reforming reaction ($R30$) and reverse water shift reaction ($R33$). The time averaged-time distributions of CO_2 and CH_4 mole fraction along the gasifier reactor are shown in Figure 4.15 and Figure 4.16, respectively. It is obvious that with increasing SBR, the quantities CO_2 and CH_4 inside the gasifier reactor is decreased.

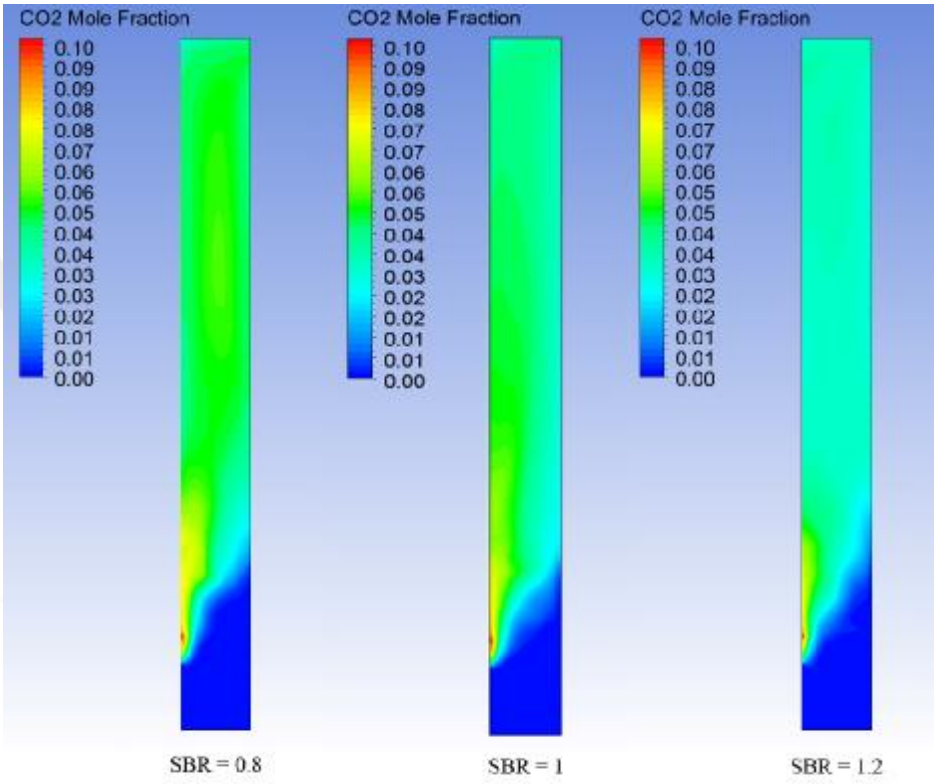

Figure 4.15. Time-averaged distribution of $\boldsymbol{CO_2}$ mole fraction at $\boldsymbol{SBR}$ of 0.8, 1 and 1.2

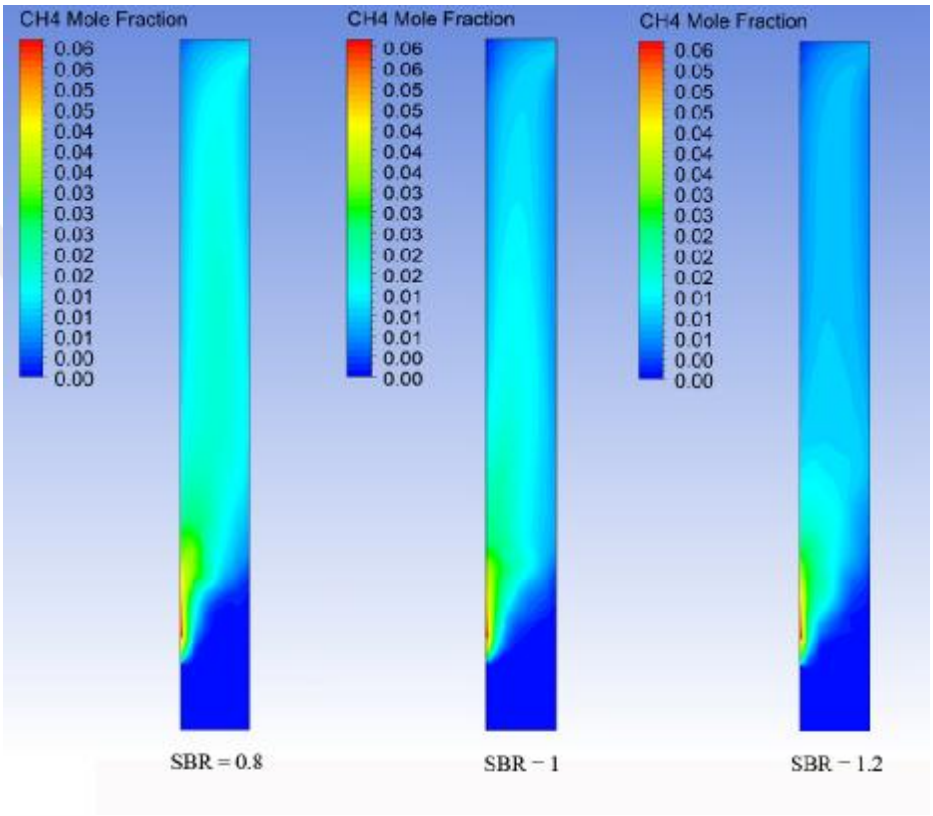

Figure 4.16. Time-averaged distribution of $\boldsymbol{CH_4}$ mole fraction at $\boldsymbol{SBR}$ of 0.8, 1 and 1.2

Since the mole fraction of CH_4 is the most influential factor on the LHV of the producer gas, LHV of the producer gas is reduced by increasing the SBR (Figure 4.17). It is observed that the influence of SBR on the producer gases is less compered to the influence of temperature (Kumar et al., 2009, Lv et al., 2007, Turn et al., 1998). In addition, with increasing SBR, char yield increases and tar content decreases. This

behavior can be seen through Figure 4.18. Furthermore, those results are in a good agreement with the results reported in (Song et al., 2012, Liu et al., 2016, Ku et al., 2015, Karmakar and Datta, 2011).

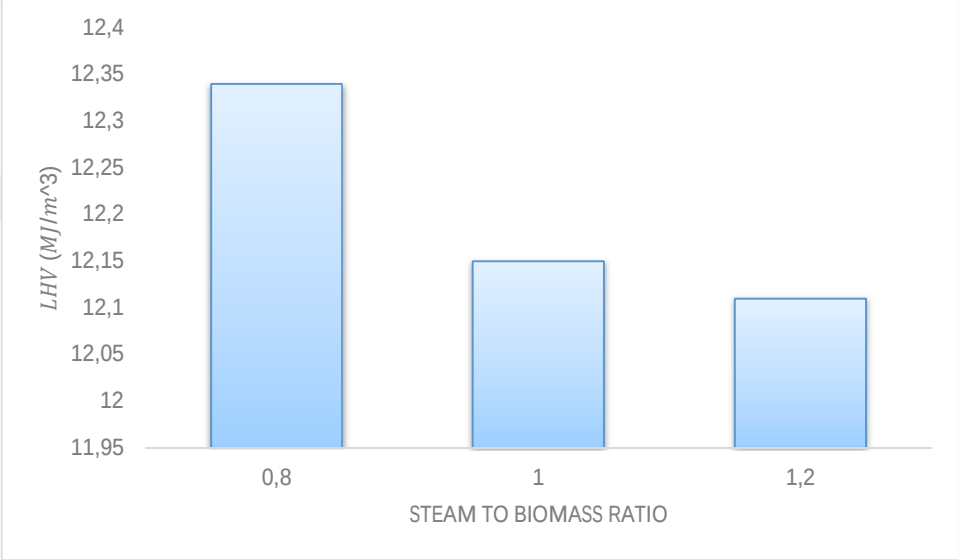

Figure 4.17. Effect of steam to biomass ratio on produced ***LHV***

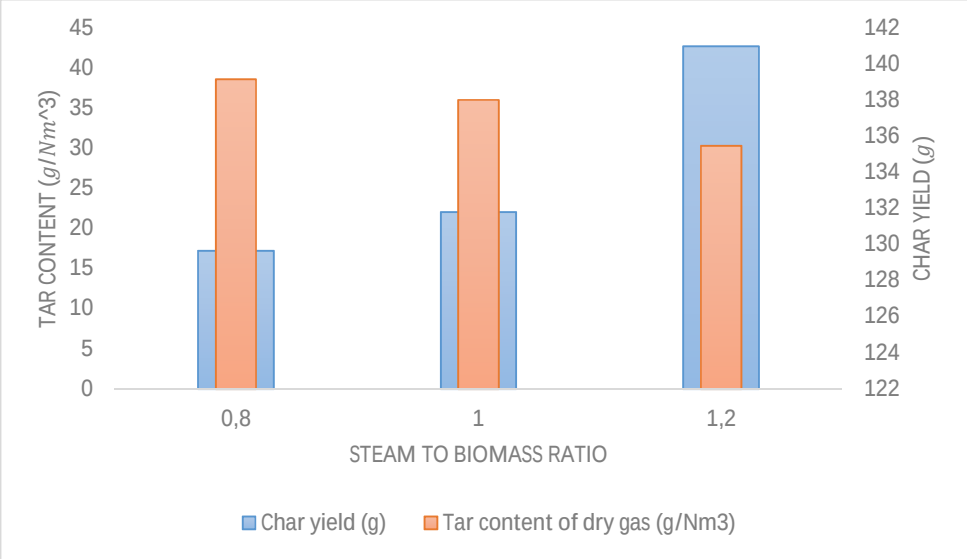

Figure 4.18. Effect of steam to biomass ratio on char yield and tar content

The effect of SBR on the tar components is not understood, however, Figure 4.19 represents the different trends of tar components with different values of SBR. Again, CH_2O and CH_3OH form the highest percentage of tar mass fraction which contribute by 39.3% (at SBR=0.8) to 38.1% (at SBR=1.2) and 36.9% (at SBR=0.8) to 37.7% (at SBR=1.2) of tar mass fraction, respectively. Meanwhile, CH_3HCO forms 12.3% (at SBR=0.8) to 13.2% (at SBR=1.2) of tar mass fraction. Furthermore, $C_6H_6O_3$ and CH_3COCH_3 are almost consumed in the tar cracking reactions when they reach the gasifier outlet.

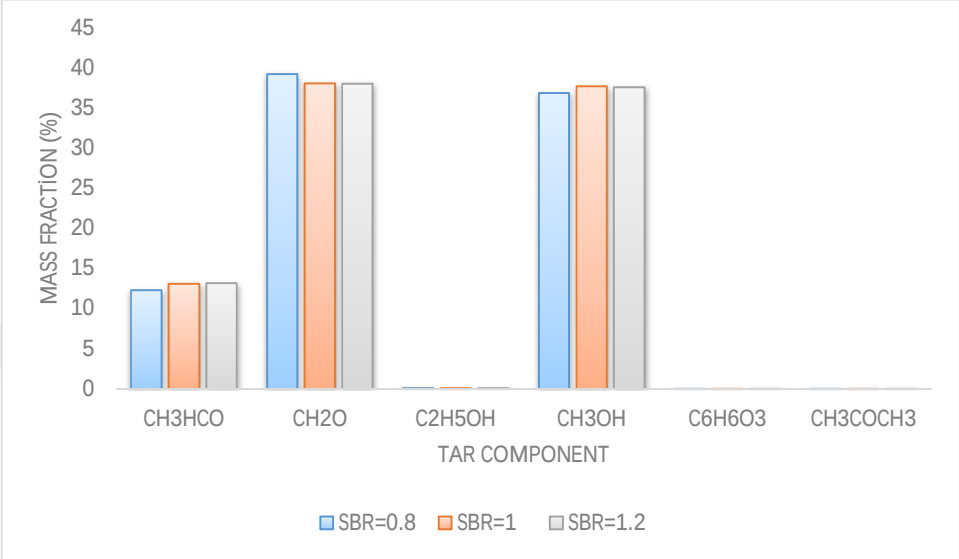

Figure 4.19 Effect of steam to biomass ratio on tar components

5. CONCLUSION

In this work, a biomass steam gasification model was developed based on comprehensive pyrolysis reaction model using ANSYS FLUENT. The multi-phase model along with granular flow kinetic theory was used to simulate the process.

The base case was validated by comparing the results gained from the current study with the experimental data (Rapagna et al., 2000) for dry syngas composition, lower heating value, and char yield. The results were accurate to a good extent, furthermore, the presented model obtained more accurate results than the previous numerical studies (Eri et al., 2018). Therefore, the model is suitable to simulate the steam gasification processes. The effect of gasification temperature as well as steam to biomass ratio on the gasification process products were analyzed in details.

The temperature of gasification showed a strong effect on syngas composition, tar content and char yield but not on the lower heating value of the syngas. By increasing the temperature, the mole fraction of H_2 and CO was increased. Meanwhile, the mole fraction of both $CH4$ and CO_2 as well as char yield decreased with the increase of temperature. The lower heating value showed a declining trend with the increase in temperature. On the other hand, steam to biomass ratio was found to has a weak influence on the producer gas but a strong influence on char yield, tar content and lower heating value. By increasing steam to biomass ratio, the mole fraction of H_2 and CO showed an inclined trend, however, the mole fraction of both CH_4 and CO_2 showed a declined trend. Char yield found to have a proportional relationship with steam to biomass ratio. However, lower heating value and tar content both both found to have a reverse relationship with steam to biomass ratio.

Furthermore, the tar components mass fraction were studied. The obtained results have a reasonable explanation which gets along with the mathematical model of tar cracking chemical reactions.

The present study filled the gap was left by the previous studies since it was able to analyze the effect of gasification temperature and steam to biomass ratio on the gasification products of almond shells. Besides, the obtained results of the base case were compared with another CFD study to prove the accuracy of the present model.

Studying the effect of equivalent ratio, height of the bed, material of the bed and geometry of gasifier reactor is recommended of future studies.

REFERENCES

AHUJA, P., KUMAR, S. & SINGH, P. C. 1996. A model for primary and heterogeneous secondary reactions of wood pyrolysis. *Chemical Engineering & Technology: Industrial Chemistry-Plant Equipment-"Process Engineering-Biotechnology,* 19**,** 272-282.

ANDERSON, T. B. & JACKSON, R. 1967. Fluid mechanical description of fluidized beds. Equations of motion. *Industrial & Engineering Chemistry Fundamentals,* 6**,** 527-539.

BARUAH, D. & BARUAH, D. C. 2014. Modeling of biomass gasification: A review. *Renewable and Sustainable Energy Reviews,* 39**,** 806-815.

BASU, P. 2010. *Biomass gasification and pyrolysis: practical design and theory*, Academic press.

BASU, P. & HALDER, P. K. 1989. Combustion of single carbon particles in a fast fluidized bed of fine solids. *Fuel,* 68**,** 1056-1063.

BLONDEAU, J. & JEANMART, H. 2012. Biomass pyrolysis at high temperatures: Prediction of gaseous species yields from an anisotropic particle. *Biomass and Bioenergy,* 41**,** 107-121.

BOROSON, M. L., HOWARD, J. B., LONGWELL, J. P. & PETERS, W. A. 1989. Product yields and kinetics from the vapor phase cracking of wood pyrolysis tars. *AIChE Journal,* 35**,** 120-128.

BUSTAMANTE, F., ENICK, R. M., CUGINI, A. V., KILLMEYER, R. P., HOWARD, B. H., ROTHENBERGER, K. S., CIOCCO, M. V., MORREALE, B. D., CHATTOPADHYAY, S. & SHI, S. 2004. High-temperature kinetics of the homogeneous reverse water-gas shift reaction. *AIChE Journal,* 50**,** 1028-1041.

BUSTAMANTE, F., ENICK, R. M., KILLMEYER, R. P., HOWARD, B. H., ROTHENBERGER, K. S., CUGINI, A. V., MORREALE, B. D. & CIOCCO, M. V. 2005. Uncatalyzed and wall-catalyzed forward water-gas shift reaction kinetics. *AIChE Journal,* 51**,** 1440-1454.

CALONACI, M., GRANA, R., BARKER HEMINGS, E., BOZZANO, G., DENTE, M. & RANZI, E. 2010. Comprehensive Kinetic Modeling Study of Bio-oil Formation from Fast Pyrolysis of Biomass. *Energy & Fuels,* 24**,** 5727-5734.

CHANG, A. C. C., CHANG, H.-F., LIN, F.-J., LIN, K.-H. & CHEN, C.-H. 2011. Biomass gasification for hydrogen production. *International Journal of Hydrogen Energy,* 36**,** 14252-14260.

CHEN, J., YU, G., DAI, B., LIU, D. & ZHAO, L. 2014. CFD Simulation of a Bubbling Fluidized Bed Gasifier Using a Bubble-Based Drag Model. *Energy & Fuels,* 28**,** 6351-6360.

COUTO, N., SILVA, V., MONTEIRO, E., TEIXEIRA, S., CHACARTEGUI, R., BOUZIANE, K., BRITO, P. S. D. & ROUBOA, A. 2015. Numerical and experimental analysis of municipal solid wastes gasification process. *Applied Thermal Engineering,* 78**,** 185-195.

DEMIRBAS, A. & ARIN, G. 2002. An overview of biomass pyrolysis. *Energy sources,* 24**,** 471-482.

DI BLASI, C. 2009. Combustion and gasification rates of lignocellulosic chars. *Progress in Energy and Combustion Science,* 35**,** 121-140.

DREW, D. A. 1983. Mathematical modeling of two-phase flow. *Annual review of fluid mechanics,* 15**,** 261-291.

ERI, Q., PENG, J. & ZHAO, X. 2018. CFD simulation of biomass steam gasification in a fluidized bed based on a multi-composition multi-step kinetic model. *Applied Thermal Engineering,* 129**,** 1358-1368.

FAGBEMI, L., KHEZAMI, L. & CAPART, R. 2001. Pyrolysis products from different biomasses: application to the thermal cracking of tar. *Applied Energy,* 69**,** 293-306.

FERREIRA, S., MOREIRA, N. A. & MONTEIRO, E. 2009. Bioenergy overview for Portugal. *Biomass and Bioenergy,* 33**,** 1567-1576.

FLETCHER, D., HAYNES, B., CHRISTO, F. & JOSEPH, S. 2000. A CFD based combustion model of an entrained flow biomass gasifier. *Applied mathematical modelling,* 24**,** 165-182.

FRANCO, C., PINTO, F., GULYURTLU, I. & CABRITA, I. 2003. The study of reactions influencing the biomass steam gasification process☆. *Fuel,* 82**,** 835-842.

GERBER, S., BEHRENDT, F. & OEVERMANN, M. 2010. An Eulerian modeling approach of wood gasification in a bubbling fluidized bed reactor using char as bed material. *Fuel,* 89**,** 2903-2917.

GIDASPOW, D. 1994. A bubbling fluidization model using kinetic theory of granular flow. *AICHE J.,* 32**,** 523-538.

GÓMEZ-BAREA, A. & LECKNER, B. 2010. Modeling of biomass gasification in fluidized bed. *Progress in Energy and Combustion Science,* 36**,** 444-509.

GUNGOR, A. 2011. Modeling the effects of the operational parameters on H2 composition in a biomass fluidized bed gasifier. *International Journal of Hydrogen Energy,* 36**,** 6592-6600.

GUNGORL, A., OZBAYOGLUZ, M., KASNAKOGLUS, C., BIYIKOGLU, A. & UYSAL, B. 2011. Gasification Process to Produce Synthesis Gas. *Journal of Environmental Science and Engineering,* 5**,** 799-804.

GUNN, D. J. 1978. Transfer of heat or mass to particles in fixed and fluidised beds. *International Journal of Heat and Mass Transfer,* 21**,** 467-476.

HUILIN, L., GIDASPOW, D., BOUILLARD, J. & WENTIE, L. 2003. Hydrodynamic simulation of gas–solid flow in a riser using kinetic theory of granular flow. *Chemical Engineering Journal,* 95**,** 1-13.

ISHII, M. & HIBIKI, T. 2010. *Thermo-fluid dynamics of two-phase flow*, Springer Science & Business Media.

ISMAIL, T. M., ABD EL-SALAM, M., MONTEIRO, E. & ROUBOA, A. 2016. Eulerian – Eulerian CFD model on fluidized bed gasifier using coffee husks as fuel. *Applied Thermal Engineering,* 106**,** 1391-1402.

ISMAIL, T. M., ABD EL-SALAM, M., MONTEIRO, E. & ROUBOA, A. 2018. Fluid dynamics model on fluidized bed gasifier using agro-industrial biomass as fuel. *Waste Manag,* 73**,** 476-486.

JONES, W. P. & LINDSTEDT, R. P. 1988. Global reaction schemes for hydrocarbon combustion. *Combustion and Flame,* 73**,** 233-249.

KARMAKAR, M. K. & DATTA, A. B. 2011. Generation of hydrogen rich gas through fluidized bed gasification of biomass. *Bioresource Technology,* 102**,** 1907-1913.

KAUSHAL, P., PROELL, T. & HOFBAUER, H. 2011. Application of a detailed mathematical model to the gasifier unit of the dual fluidized bed gasification plant. *Biomass and Bioenergy,* 35**,** 2491-2498.

KERN, S., PFEIFER, C. & HOFBAUER, H. 2013. Gasification of wood in a dual fluidized bed gasifier: Influence of fuel feeding on process performance. *Chemical Engineering Science,* 90**,** 284-298.

KIRKELS, A. F. & VERBONG, G. P. J. 2011. Biomass gasification: Still promising? A 30-year global overview. *Renewable and Sustainable Energy Reviews,* 15**,** 471-481.

KıRTAY, E. 2011. Recent advances in production of hydrogen from biomass. *Energy Conversion and Management,* 52**,** 1778-1789.

KU, X., LI, T. & LØVÅS, T. 2013. Influence of drag force correlations on periodic fluidization behavior in Eulerian–Lagrangian simulation of a bubbling fluidized bed. *Chemical Engineering Science,* 95**,** 94-106.

KU, X., LI, T. & LØVÅS, T. 2015. CFD–DEM simulation of biomass gasification with steam in a fluidized bed reactor. *Chemical Engineering Science,* 122**,** 270-283.

KUMAR, A., ESKRIDGE, K., JONES, D. D. & HANNA, M. A. 2009. Steam–air fluidized bed gasification of distillers grains: Effects of steam to biomass ratio, equivalence ratio and gasification temperature. *Bioresource Technology,* 100**,** 2062-2068.

LI, X., GRACE, J. R., WATKINSON, A. P., LIM, C. J. & ERGÜDENLER, A. 2001. Equilibrium modeling of gasification: a free energy minimization approach and its application to a circulating fluidized bed coal gasifier. *Fuel,* 80**,** 195-207.

LI, X. T., GRACE, J. R., LIM, C. J., WATKINSON, A. P., CHEN, H. P. & KIM, J. R. 2004. Biomass gasification in a circulating fluidized bed. *Biomass and Bioenergy,* 26**,** 171-193.

LITTLEWOOD, K. 1977. Gasification: Theory and application. *Progress in Energy and Combustion Science,* 3**,** 35-71.

LIU, H., CATTOLICA, R. J. & SEISER, R. 2016. CFD studies on biomass gasification in a pilot-scale dual fluidized-bed system. *International Journal of Hydrogen Energy,* 41**,** 11974-11989.

LIU, H., HU, J., WANG, H., WANG, C. & LI, J. 2012. Experimental studies of biomass gasification with air. *Journal of Natural Gas Chemistry,* 21**,** 374-380.

LOHA, C., CHATTOPADHYAY, H. & CHATTERJEE, P. K. 2012. Assessment of drag models in simulating bubbling fluidized bed hydrodynamics. *Chemical Engineering Science,* 75**,** 400-407.

LV, P., YUAN, Z., WU, C., MA, L., CHEN, Y. & TSUBAKI, N. 2007. Bio-syngas production from biomass catalytic gasification. *Energy Conversion and Management,* 48**,** 1132-1139.

MELLIN, P., KANTARELIS, E. & YANG, W. 2014. Computational fluid dynamics modeling of biomass fast pyrolysis in a fluidized bed reactor, using a comprehensive chemistry scheme. *Fuel,* 117**,** 704-715.

NIKOO, M. B. & MAHINPEY, N. 2008. Simulation of biomass gasification in fluidized bed reactor using ASPEN PLUS. *Biomass and Bioenergy,* 32**,** 1245-1254.

PAPADIKIS, K., GU, S. & BRIDGWATER, A. V. 2010. A CFD approach on the effect of particle size on char entrainment in bubbling fluidised bed reactors. *Biomass and Bioenergy,* 34**,** 21-29.

PARK, W. C., ATREYA, A. & BAUM, H. R. 2010. Experimental and theoretical investigation of heat and mass transfer processes during wood pyrolysis. *Combustion and Flame,* 157**,** 481-494.

PHILLIPS, J. 2006. Different types of gasifiers and their integration with gas turbines. *The gas turbine handbook,* 1.

QI, T., LEI, T., YAN, B., CHEN, G., LI, Z., FATEHI, H., WANG, Z. & BAI, X.-S. 2019. Biomass steam gasification in bubbling fluidized bed for higher-H2 syngas: CFD simulation with coarse grain model. *International Journal of Hydrogen Energy,* 44**,** 6448-6460.

RADMANESH, R., CHAOUKI, J. & GUY, C. 2006. Biomass gasification in a bubbling fluidized bed reactor: experiments and modeling. *AIChE Journal,* 52**,** 4258-4272.

RANZI, E., CUOCI, A., FARAVELLI, T., FRASSOLDATI, A., MIGLIAVACCA, G., PIERUCCI, S. & SOMMARIVA, S. 2008. Chemical kinetics of biomass pyrolysis. *Energy & Fuels,* 22**,** 4292-4300.

RAPAGNA, S., JAND, N., KIENNEMANN, A. & FOSCOLO, P. U. 2000. Steam-gasification of biomass in a fluidised-bed of olivine particles. *Biomass and bioenergy,* 19**,** 187-197.

SANDE, P. C. & RAY, S. 2014. Mesh size effect on CFD simulation of gas-fluidized Geldart A particles. *Powder Technology,* 264**,** 43-53.

SCHUSTER, G., LÖFFLER, G., WEIGL, K. & HOFBAUER, H. 2001. Biomass steam gasification – an extensive parametric modeling study. *Bioresource Technology,* 77**,** 71-79.

SHADLE, L. J., BERRY, D. A. & SYAMLAL, M. 2000. Coal conversion processes, gasification. *Kirk-Othmer Encyclopedia of Chemical Technology*.

SHEN, L., GAO, Y. & XIAO, J. 2008. Simulation of hydrogen production from biomass gasification in interconnected fluidized beds. *Biomass and Bioenergy,* 32**,** 120-127.

SIKARWAR, V. & ZHAO, M. 2017. Biomass Gasification.

SNIDER, D. M., CLARK, S. M. & O'ROURKE, P. J. 2011. Eulerian–Lagrangian method for three-dimensional thermal reacting flow with application to coal gasifiers. *Chemical Engineering Science,* 66**,** 1285-1295.

SONG, T., WU, J., SHEN, L. & XIAO, J. 2012. Experimental investigation on hydrogen production from biomass gasification in interconnected fluidized beds. *Biomass and Bioenergy,* 36**,** 258-267.

SUSASTRIAWAN, A. A. P., SAPTOADI, H. & PURNOMO 2017. Small-scale downdraft gasifiers for biomass gasification: A review. *Renewable and Sustainable Energy Reviews,* 76**,** 989-1003.

TOMIYAMA, A. 1998. Struggle with computational bubble dynamics. *Multiphase Science and Technology,* 10**,** 369-405.

TURN, S., KINOSHITA, C., ZHANG, Z., ISHIMURA, D. & ZHOU, J. 1998. An experimental investigation of hydrogen production from biomass gasification. *International Journal of Hydrogen Energy,* 23**,** 641-648.

WANG, Z., HE, T., QIN, J., WU, J., LI, J., ZI, Z., LIU, G., WU, J. & SUN, L. 2015. Gasification of biomass with oxygen-enriched air in a pilot scale two-stage gasifier. *Fuel,* 150**,** 386-393.

WANG, X., JIN, B. & ZHONG, W. 2009. Three-dimensional simulation of fluidized bed coal gasification. *Chemical Engineering and Processing: Process Intensification,* 48**,** 695-705.

XIE, J., ZHONG, W., JIN, B., SHAO, Y. & LIU, H. 2012. Simulation on gasification of forestry residues in fluidized beds by Eulerian-Lagrangian approach. *Bioresour Technol,* 121**,** 36-46.

XIE, J., ZHONG, W., JIN, B., SHAO, Y. & LIU, H. 2014. Three-Dimensional Eulerian–Eulerian Modeling of Gaseous Pollutant Emissions from Circulating Fluidized-Bed Combustors. *Energy & Fuels,* 28**,** 5523-5533.

XUE, Q. & FOX, R. O. 2014. Multi-fluid CFD modeling of biomass gasification in polydisperse fluidized-bed gasifiers. *Powder Technology,* 254**,** 187-198.

YANG, H., YAN, R., CHEN, H., LEE, D. H. & ZHENG, C. 2007. Characteristics of hemicellulose, cellulose and lignin pyrolysis. *Fuel,* 86**,** 1781-1788.

ZHOU, H., JENSEN, A. D., GLARBORG, P., JENSEN, P. A. & KAVALIAUSKAS, A. 2005. Numerical modeling of straw combustion in a fixed bed. *Fuel,* 84**,** 389-403.